Please cite this article in press as: Haack et al., Absence of the Autophagy Adaptor SQSTM1/p62 Causes Childhood-Onset Neurodegeneration with Ataxia, Dystonia, and Gaze Palsy, The American Journal of Human Genetics (2016), http://dx.doi.org/10.1016/j.ajhg.2016.06.026

REPORT

Absence of the Autophagy Adaptor SQSTM1/p62 Causes Childhood-Onset Neurodegeneration with Ataxia, Dystonia, and Gaze Palsy

Tobias B. Haack,[1,2,22,*] Erika Ignatius,[3,4,22] Javier Calvo-Garrido,[5,22] Arcangela Iuso,[1,2,22] Pirjo Isohanni,[3,4] Camilla Maffezzini,[6] Tuula Lönnqvist,[4] Anu Suomalainen,[3] Matteo Gorza,[2] Laura S. Kremer,[1,2] Elisabeth Graf,[2] Monika Hartig,[1] Riccardo Berutti,[2] Martin Paucar,[7] Per Svenningsson,[7] Henrik Stranneheim,[5,8] Göran Brandberg,[9] Anna Wedell,[5,8] Manju A. Kurian,[10,11] Susan A. Hayflick,[12,13,14] Paola Venco,[15] Valeria Tiranti,[15] Tim M. Strom,[1,2] Martin Dichgans,[16,17,18] Rita Horvath,[19,20] Elke Holinski-Feder,[19] Christoph Freyer,[6,8] Thomas Meitinger,[1,2,17] Holger Prokisch,[1,2,22] Jan Senderek,[21,22] Anna Wredenberg,[6,8,22] Christopher J. Carroll,[3,22] and Thomas Klopstock[17,18,21,22,*]

SQSTM1 (sequestosome 1; also known as *p62*) encodes a multidomain scaffolding protein involved in various key cellular processes, including the removal of damaged mitochondria by its function as a selective autophagy receptor. Heterozygous variants in *SQSTM1* have been associated with Paget disease of the bone and might contribute to neurodegeneration in amyotrophic lateral sclerosis (ALS) and frontotemporal dementia (FTD). Using exome sequencing, we identified three different biallelic loss-of-function variants in *SQSTM1* in nine affected individuals from four families with a childhood- or adolescence-onset neurodegenerative disorder characterized by gait abnormalities, ataxia, dysarthria, dystonia, vertical gaze palsy, and cognitive decline. We confirmed absence of the SQSTM1/p62 protein in affected individuals' fibroblasts and found evidence of a defect in the early response to mitochondrial depolarization and autophagosome formation. Our findings expand the *SQSTM1*-associated phenotypic spectrum and lend further support to the concept of disturbed selective autophagy pathways in neurodegenerative diseases.

Neurodegenerative disease causes severe disability or even early death and many families and affected individuals remain without a specific molecular diagnosis. The identification of underlying gene defects in both common and rare conditions provided fundamental new insights into pathophysiology and basic cellular processes. Examples are the discovery of gene defects underlying Parkinson disease (PD) and amyotrophic lateral sclerosis (ALS). Proteins encoded by affected genes such as PARKIN (PARK2), PINK1, OPTN, SQSTM1/p62, and TBK1 offer a new perspective on the involvement of mitochondria. Specifically, these proteins are thought to be involved in the maintenance of a functioning pool of mitochondria by regulating their turnover by selective autophagocytic processes.[1,2] One recent model suggests that after loss of mitochondrial membrane potential or accumulation of misfolded proteins, PINK1 generates a phospho-ubiquitin signature on mitochondria to induce recruitment of the primary autophagy adaptors OPTN and NDP52, which then engage with the autophagy machinery (ULK1, DFCP1, WIPI1, and LC3).[3] Although TBK1-dependent phosphorylation of OPTN and NDP52 is thought to be crucial for robust mitophagy, the presence of additional/alternative autophagy adaptors such as TAX1BP1, NRB1, and SQSTM1/p62 is dispensable for mitophagy itself.[3]

In addition to its function in autophagy, the multidomain scaffold protein SQSTM1/p62 plays a role in diverse other key cellular pathways; heterozygous *SQSTM1* (MIM: 601530) variants have been suggested to contribute to the pathogenesis of such diverse presentations as Paget disease of the bone (PDB [MIM: 167250]), ALS, FTD (MIM: 616437),[4] and recently distal myopathy with

[1]Institute of Human Genetics, Technische Universität München, 81675 Munich, Germany; [2]Institute of Human Genetics, Helmholtz Zentrum München, 85764 Neuherberg, Germany; [3]Research Programs Unit, Molecular Neurology, University of Helsinki, 00290 Helsinki, Finland; [4]Department of Child Neurology, Children's Hospital, University of Helsinki and Helsinki University Hospital, 00029 HUS, Finland; [5]Department of Molecular Medicine and Surgery, Science for Life Laboratory, Karolinska Institutet, Stockholm 17176, Sweden; [6]Department of Medical Biochemistry and Biophysics, Karolinska Institutet, Stockholm 17177, Sweden; [7]Department of Clinical Neuroscience, Karolinska Institutet, Stockholm 17176, Sweden; [8]Centre for Inherited Metabolic Diseases, Karolinska University Hospital, Stockholm 17176, Sweden; [9]Department of Pediatrics, Falu lasarett, 79182 Falun, Sweden; [10]Neurosciences Unit, Institute of Child Health, University College London, London WC1N 3BG, UK; [11]Department of Paediatric Neurology, Great Ormond Street Hospital, London WC1N 3BG, UK; [12]Department of Pediatrics, Oregon Health & Science University, Portland, OR 97239, USA; [13]Department of Molecular & Medical Genetics, Oregon Health & Science University, Portland, OR 97239, USA; [14]Department of Neurology, Oregon Health & Science University, Portland, OR 97239, USA; [15]Unit of Molecular Neurogenetics – Pierfranco and Luisa Mariani Center for the study of Mitochondrial Disorders in Children, IRCCS Foundation Neurological Institute "C. Besta," 20126 Milan, Italy; [16]Institute for Stroke and Dementia Research, Ludwig-Maximilians-University of Munich, 81377 Munich, Germany; [17]Munich Cluster for Systems Neurology (SyNergy), 80336 Munich, Germany; [18]DZNE - German Center for Neurodegenerative Diseases, 80336 Munich, Germany; [19]MGZ - Medical Genetics Center, 80335 Munich, Germany; [20]Institute of Genetic Medicine, MRC Centre for Neuromuscular Diseases, Newcastle University, Newcastle upon Tyne NE1 3BZ, UK; [21]Department of Neurology, Friedrich-Baur-Institute, Ludwig-Maximilians-University, 80336 Munich, Germany
[22]These authors contributed equally to this work
*Correspondence: tobias.haack@helmholtz-muenchen.de (T.B.H.), tklopsto@med.lmu.de (T.K.)
http://dx.doi.org/10.1016/j.ajhg.2016.06.026.

Please cite this article in press as: Haack et al., Absence of the Autophagy Adaptor SQSTM1/p62 Causes Childhood-Onset Neurodegeneration with Ataxia, Dystonia, and Gaze Palsy, The American Journal of Human Genetics (2016), http://dx.doi.org/10.1016/j.ajhg.2016.06.026

Table 1. Genetic and Clinical Findings in Individuals with Biallelic *SQSTM1* Loss-of-Function Variants

		SQSTM1 Variants	Phenotypic Features									MRI Findings	
ID	Sex	cDNA (NM_003900.4), Protein (NP_003891.1)	AaO[a]	AaLE[a]	Gait Abn.	Ataxia	Dystonia	Dysarthria	Gaze Palsy	MND	Cognitive Decline	CA	Iron
F1:II.1	M	c.[2T>A];[2T>A], p.[?];[?]	10	45	+*	+*	+	+	+	+L	–	ND	ND
F1:II.3	F	c.[2T>A];[2T>A], p.[?];[?]	12	42	+*	+	+	+	+	+U/L	+*	–	+
F1:II.6	F	c.[2T>A];[2T>A], p.[?];[?]	15	33	+*	+*	+	+	–	–	+	–	+
F2:II.2	F	c.[311_312del];[311_312del], p.[Glu104Valfs48*];[Glu104Valfs48*]	10	31	+*	+*	+	+	+	–	+*	+	–
F2:II.3	F	c.[311_312del];[311_312del], p.[Glu104Valfs48*];[Glu104Valfs48*]	10	18	+*	+*	+	(+)	+	–	+*	+	–
F2:II.z	F	c.[311_312del];[311_312del], p.[Glu104Valfs48*];[Glu104Valfs48*]	10	12	+*	+*	+	(+)	+	–	+*	+	–
F3:II.1	F	c.[286C>T];[286C>T], p.[Arg96*];[Arg96*]	7	18	+*	+*	–	+*	–	–	+	+	–
F4:II.1	F	c.[286C>T];[286C>T], p.[Arg96*];[Arg96*]	8	33	+	+*	–	+	+	–	+	–	–
F4:II.4	M	c.[286C>T];[286C>T], p.[Arg96*];[Arg96*]	8	17	+	+*	+	+	+	–	+	–	–

Abbreviations are as follows: AaLE, age at last examination; AaO, age at onset; abn., abnormalities; CA, cerebellar atrophy; MND, motor neuron disorder (L, lower MND; U/L, upper and lower MND); ND, not done; *, among the presenting symptoms; +, affected; (+), mildly affected; –, not affected.
[a]Ages in years.

rimmed vacuoles.[5] Here, we report on the phenotypic spectrum associated with absence of SQSTM1/p62 as well as the results of our studies of mitophagy-related phenotypes in mutant fibroblast cell lines.

We performed exome sequencing on genomic DNA from affected individuals from four families with a so far etiologically unresolved childhood- or adolescence-onset neurodegenerative syndrome manifesting with gait abnormalities and ataxia. Clinical and genetic findings are summarized in Table 1, pedigrees are shown in Figure 1, and neuroimaging findings are in Figure 2. A summary of the phenotypes is provided below, and the detailed individual case reports are provided in the Supplemental Data. Informed consent was obtained from all affected individuals or their guardians. The study was approved by the local ethics committees.

Family 1 consists of three affected siblings, one male (F1:II.1) and two females (F1:II.3, F1:II.6), and three healthy siblings born to healthy unrelated parents of German origin. All affected individuals presented with gait problems in their early teen years, progressing to wheelchair dependence at ages 16–32 years. Other presenting symptoms included urinary incontinence, upper limb ataxia, and cognitive decline. Last clinical examination at ages 45, 42, and 33 years, respectively, revealed generalized dystonia, dysarthria, and a cerebellar syndrome in all three affected siblings, as well as vertical gaze palsy and a pyramidal syndrome in two. None had a history of psychiatric symptoms, seizures, tremor, or visual impairment. Brain MRI showed accumulation of iron in basal ganglia in individuals F1:II.3 and F1:II.6 (Figure 2). A muscle biopsy in F1:II.6 was unremarkable regarding morphology, histochemistry, ultrastructure, and mitochondrial enzyme analysis.

Family 2 consists of three affected sisters (F2:II.2, F2:II.3, F2:II.4) and nine reportedly healthy siblings, born to healthy parents from the United Arab Emirates who were unaware of consanguinity. All affected siblings had a remarkably similar course with unsteadiness of gait, coordination problems, and cognitive decline from the age of 10 years. At last clinical examination at ages 31, 18, and 12 years, respectively, all were still able to walk independently but showed short and thin stature, a cerebellar syndrome, marked vertical gaze palsy, hearing loss, and a dystonic or athetotic movement disorder. Brain MRI showed mild cerebellar atrophy in all affected siblings (Figure 2).

Family 3 consists of one affected sister (F3:II.1) and one healthy brother, born to healthy unrelated parents from Finland. The affected sister presented at the age of 7 years with tremor, oculomotor apraxia, and dysarthria. Last clinical examination at age 18 years showed a cerebellar syndrome and cognitive impairment. Brain MRI revealed mild to moderate cerebellar atrophy (Figure 2). Muscle biopsy was unremarkable regarding morphology, histochemistry, and ultrastructure but respiratory chain enzyme analysis showed a slight decrease in complex IV activity.

Please cite this article in press as: Haack et al., Absence of the Autophagy Adaptor SQSTM1/p62 Causes Childhood-Onset Neurodegeneration with Ataxia, Dystonia, and Gaze Palsy, The American Journal of Human Genetics (2016), http://dx.doi.org/10.1016/j.ajhg.2016.06.026

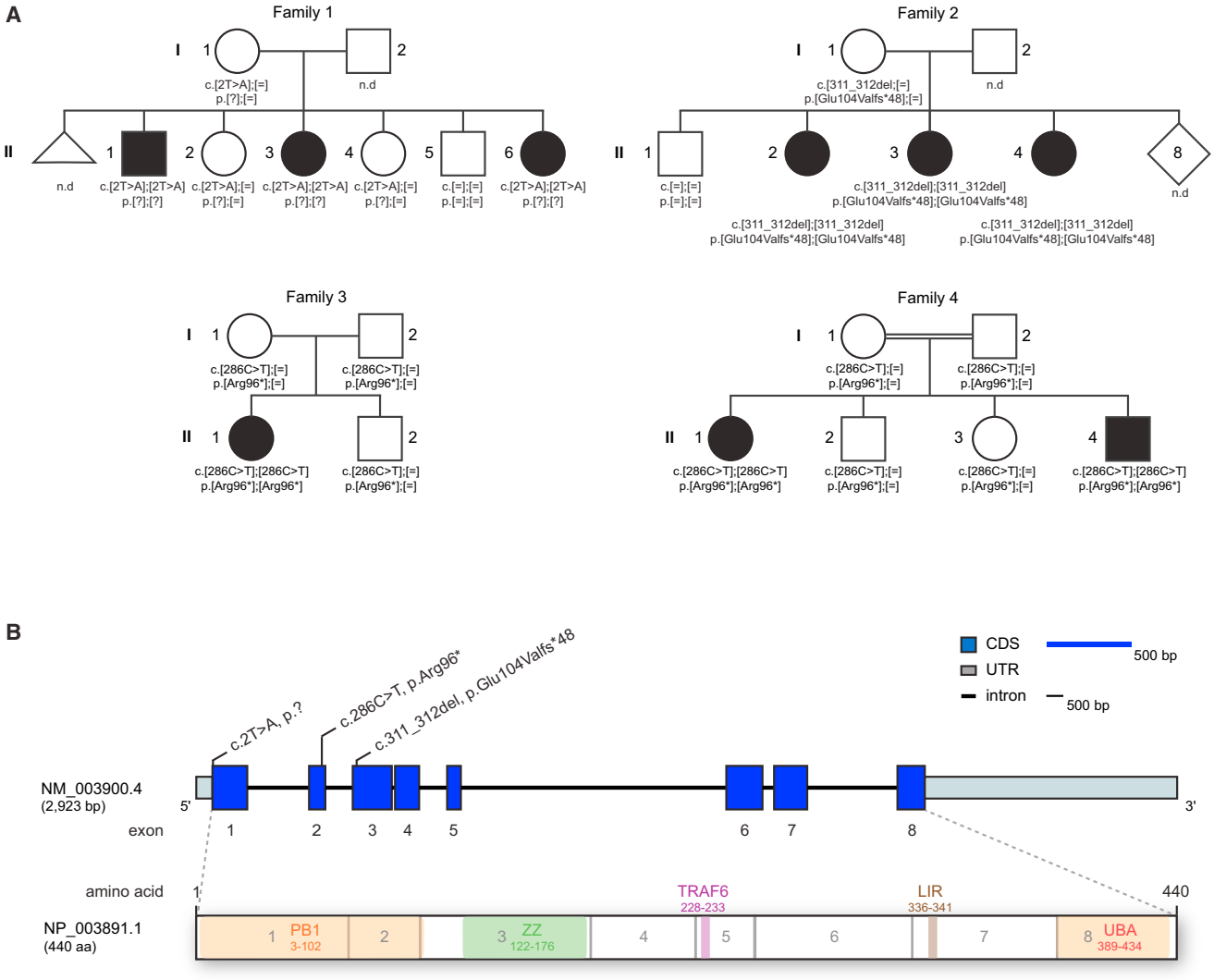

Figure 1. Pedigrees of Investigated Families and Structure of *SQSTM1*

(A) Pedigrees of four families with mutations in *SQSTM1*. Mutation status of affected (closed symbols) and healthy (open symbols) family members. n.d., not determined.

(B) Gene structure of *SQSTM1* with known protein domains and motifs of the gene product and localization of the identified mutations. Intronic regions are not drawn to scale. Abbreviations are as follows: PB1, Phox 1 and Bem1p; ZZ, zinc finger; TRAF6, tumor necrosis factor receptor-associated factor 6; LIR, LC3-interaction region; KIR, Keap1-interacting; UBA, ubiquitin-associated.

Family 4 consists of two affected individuals, one female (F4:II.1) and one male (F4:II.4), and two healthy siblings, born to healthy consanguineous parents of Kurdish descent. Both affected siblings presented at the age of 8 years with a syndrome of ataxia, dysarthria, and vertical gaze palsy. Last clinical examination at ages 33 and 17 years, respectively, revealed a cerebellar syndrome and cognitive impairment. Although F4:II.1 is still walking with a broad-based gait at age 33 years, her brother (F4:II.4) is wheelchair bound at age 17 years. Brain MRI and EEG showed normal findings in both. In F4:II:4, mitochondrial ATP production rate and respiratory chain enzyme activities were toward the lower end of normal, with complex IV activity being mostly affected. In agreement with this, fibroblasts grown on galactose as carbon source showed a mild complex IV defect (Figure S1).

We performed exome sequencing at three centers (Munich [families 1 and 2], Helsinki [family 3], and Stockholm [family 4]) on genomic DNA from three affected individuals of family 1, individuals F2:II.2 and F3:II.1, as well as on both affected individuals and their parents of family 4, essentially as described previously.[6]

In family 1, individuals F1:II.1 and F1:II.3 have been investigated in a prior experiment with a SureSelect Human All Exon 38 Mb enrichment kit (Illumina). A search for recessive-type non-synonymous variants with a minor allele frequency (MAF) < 0.1% in an in-house database containing 7,000 control exomes and the Exome Aggregation Consortium (ExAC) Server (09/2015) failed to prioritize likely pathogenic variants common to both individuals. We speculated that we had missed the responsible variant due to insufficient coverage of target sequences and

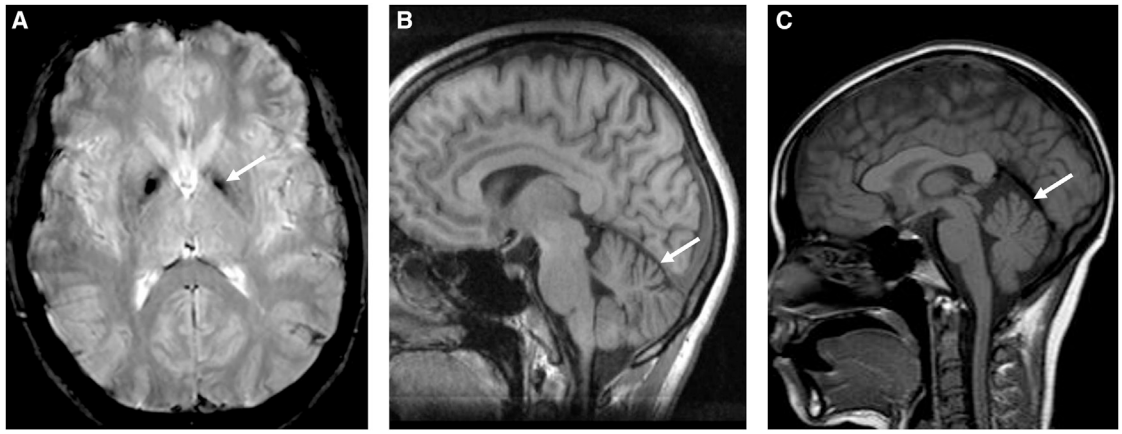

Figure 2. Neuroimaging Findings in SQSTM1/p62 Variant Individuals
(A) Brain MRI (T2-weighted image, axial view) of individual F1:II.6 at the age of 33 years, demonstrating iron accumulation in the globus pallidus internus.
(B) Brain MRI (T1-weighted image, sagittal view) of individual F2:II.2 at the age of 31 years, demonstrating mild cerebellar atrophy.
(C) Brain MRI (T1-weighted image, sagittal view) of individual F3:II.1 at the age of 18 years showing mild to moderate upper vermian atrophy.

processed DNA of the third affected individual (F1:II.6) with an updated version of the enrichment kit, SureSelect Human All Exon 50 Mb V3, potentially providing an improved coverage of the coding regions. This analysis identified seven genes carrying potential compound heterozygous or homozygous variants, with *SQSTM1* being the only gene carrying two predicted loss-of-function alleles (Table S1). Manual inspection of the sequencing data confirmed that the *SQSTM1* (GenBank: NM_003900.4) variant c.2T>A (p.?) in exon 1 was missed as an alternative call in the exome datasets of the two other siblings due to insufficient coverage of this genomic position, which reflects a general problem of GC-rich first exons. Subsequent Sanger sequencing confirmed the c.2T>A variant in a homozygous state in all affected individuals, with the mother and healthy siblings being heterozygotes or wild-types. These results were in line with the observation that the *SQSTM1* locus is located within one of six regions of interest of a previously performed SNP-array linkage study performed on this family. Because no paternal samples were available for carrier testing, we cannot exclude a large deletion on the paternal chromosome. However, analysis of the gene dosage in individual F1:II.6's exome dataset using exome depth as described previously did not indicate any copy-number variation.[7,8]

In individual F2:II.2, sequencing was performed using a SureSelect Human All Exon 38 Mb enrichment kit. A search for genes carrying putative compound heterozygous or homozygous rare variants identified 30 candidate genes, 7 of which were affected by variants rated likely detrimental in silico (see Table S1). Segregation analysis by Sanger sequencing on DNAs of further family members excluded a likely clinical relevance of variants in five putative candidate genes, leaving a homozygous frameshift variant c.311_312del (p.Glu104Valfs*48) in *SQSTM1* as the likely candidate. No material was available to confirm a heterozygous carrier status of the father. However, we did not detect any evidence of a large heterozygous deletion in the exome data of individual F2:II.2.[8]

In individual F3:II.1, the exome targets of the affected individual's DNA were captured with the Agilent SureSelect Human All Exon V5 whole exome kit followed by sequencing with the Illumina HiSeq 2000 platform. The variant calling pipeline of the Finnish Institute of Molecular Medicine (FIMM) was used for the reference genome alignment and variant calling.[9] Variants with a Combined Annotation Dependent Depletion (CADD) C-score less than 10 were excluded.[10] A search for recessive-type nonsynonymous variants with a MAF $< 0.1\%$ on the ExAC Server (09/2015) prioritized three candidate genes: *LLGL1* (MIM: 600966), *RYR1* (MIM: 180901), and *SQSTM1*. Variants in *RYR1* have been associated with unrelated autosomal-recessive inherited phenotypes (MIM: 255320 and 117000). Variants in *LLGL1* have so far not been associated with human disease and although an effect of the predictively synonymous variant on splicing cannot be excluded, we considered it unlikely to be associated with the disease of individual F3:II.1. A homozygous *SQSTM1* loss-of-function variant with a CADD score of 45, c.286C>T (p.Arg96*), remained as the top scoring candidate.

Family 4 was sequenced on the Hiseq 2500 platform (Illumina) using the Agilent SureSelect Human All Exon V4 whole exome kit. The resulting sequences were analyzed using an in-house Mutation Identification Pipeline (MIP) as previously described.[11] All called variants are scored and ranked using the Mutation Identification Pipeline weighted sum model, which uses multiple parameters but emphasizes Mendelian inheritance patterns, conserved, rare, and protein-damaging variants. This left a homozygous c.286C>T (p.Arg96*) *SQSTM1* loss-of-function variant as the top-scoring variant. Sanger sequencing of parents and affected siblings confirmed that the

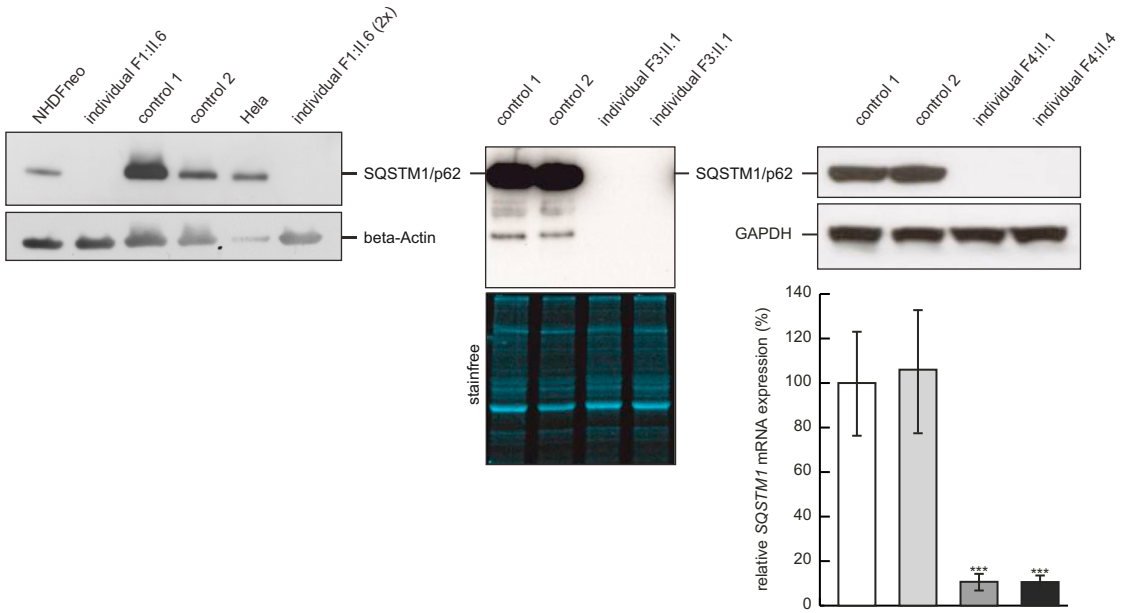

Figure 3. Investigation of SQSTM1/p62 Protein and RNA Levels
Western blot studies in SQSTM1/p62 variant fibroblast cell lines indicating that the homozygous variants c.2T>A (p.?) and c.286C>T (p.Arg96*) result in a loss of SQSTM1/p62 protein. Immunoblotting was done with anti-SQSTM1/p62 antibody (F1:II.6 with Progen cat# GP62-C; F3:II.1 and F4:II.1,4 with Cell Signaling cat# 5114).
In SQSTM1/p62 variant fibroblasts cell lines of F4:II.1,4, total RNA was isolated for qPCR analysis using Trizol. Reverse transcription for qRT-PCR analysis was performed using High Capacity cDNA Reverse Transcription Kit (Life Technologies). qRT-PCR was performed on a QuantStudio 6 (Life Technologies) with Platinum SYBR Green qPCR supermix-UDG (Life Technologies) and gene-specific primers. Error bars indicate ± SEM; ***$p \leq 0.001$; two-tailed unpaired t test. The first two columns refer to controls 1 and 2, and the last two columns refer to affected individuals F4:II.1 and F4:II.4.

SQSTM1 variant co-segregated with the phenotype in line with autosomal-recessive inheritance.

Biallelic loss-of-function *SQSTM1* variants were absent from 7,000 in-house exomes (Munich) of individuals with unrelated phenotypes and no such homozygous variants were observed in ~120,000 alleles of the ExAC Server (09/2015). Western blot studies in primary fibroblasts available from individuals F1:II.6, F3.II.1, F4:II.1, and F4:II.4 showed absence of the SQSTM1/p62 protein accompanied by a severe reduction in *SQSTM1* mRNA steady-state levels in fibroblasts from individuals F4:II.1 and F4:II.4 (Figure 3). In summary, the identification of three different biallelic *SQSTM1* loss-of-function variants in four unrelated families with a similar clinical phenotype establishes *SQSTM1* as a gene confidently implicated in this neurodegenerative disease. The identified variants c.286C>T (p.Arg96*) and c.311_312del (p.Glu104Valfs*48) affect all three predicted *SQSTM1* isoforms. In contrast, the variant c.2T>A (p.?) affects only the start codon of one out of three predicted isoforms, and while arguing for the importance of this isoform in the pathogenesis of the disease, it raises the possibility of residual mRNA/protein amount. RNA sequencing in fibroblasts and whole blood suggested partial expression of the two other isoforms (Figure S2). However, the antibody directed against the C terminus of the SQSTM1/p62 protein common to all three isoforms failed to provide evidence of any translated *SQSTM1* gene products, at least in fibroblasts.

The mutation c.286C>T has been detected in families F3 and F4. In order to test for the possibility of a shared ancestral change, we compared the variation observed in the ~2 Mb region surrounding the variant. Identified rare (MAF < 1% in public databases) variants were not shared between subjects of families 3 and 4 carrying the c.286C>T variant, indicating that this is unlikely a single ancestral variant but arose independently in the two families, in line with the reportedly Finnish and Kurdish descent of families 3 and 4, respectively.

The scaffold protein SQSTM1/p62 is highly conserved among metazoans and was originally identified as a signal adaptor for the atypical protein kinases C sub-family (aPKCs).[12,13] SQSTM1/p62 serves as a signaling hub in a variety of key cellular processes such as cell differentiation, cell growth, osteoclastogenesis, tumorigenesis, amino acid sensing, and oxidative stress response.[14,15] Its interactions with binding partners are mediated by multiple domains (Figure 1). SQSTM1/p62 is found in different compartments of the cell including the cytoplasm, nucleus, autophagosomes, and lysosomes. Upon stress induction, SQSTM1/p62 is activated to enable selective autophagy, e.g., of cells infected by bacteria, protein aggregates, and damaged mitochondria.[16–20] Earlier studies had suggested that SQSTM1/p62 is responsible for the PARKIN-mediated direction of ubiquitinated mitochondria to the autophagosome.[17] However, growing evidence indicates that SQSTM1/p62 is not essential for mitophagy itself[3,18] but

Please cite this article in press as: Haack et al., Absence of the Autophagy Adaptor SQSTM1/p62 Causes Childhood-Onset Neurodegeneration with Ataxia, Dystonia, and Gaze Palsy, The American Journal of Human Genetics (2016), http://dx.doi.org/10.1016/j.ajhg.2016.06.026

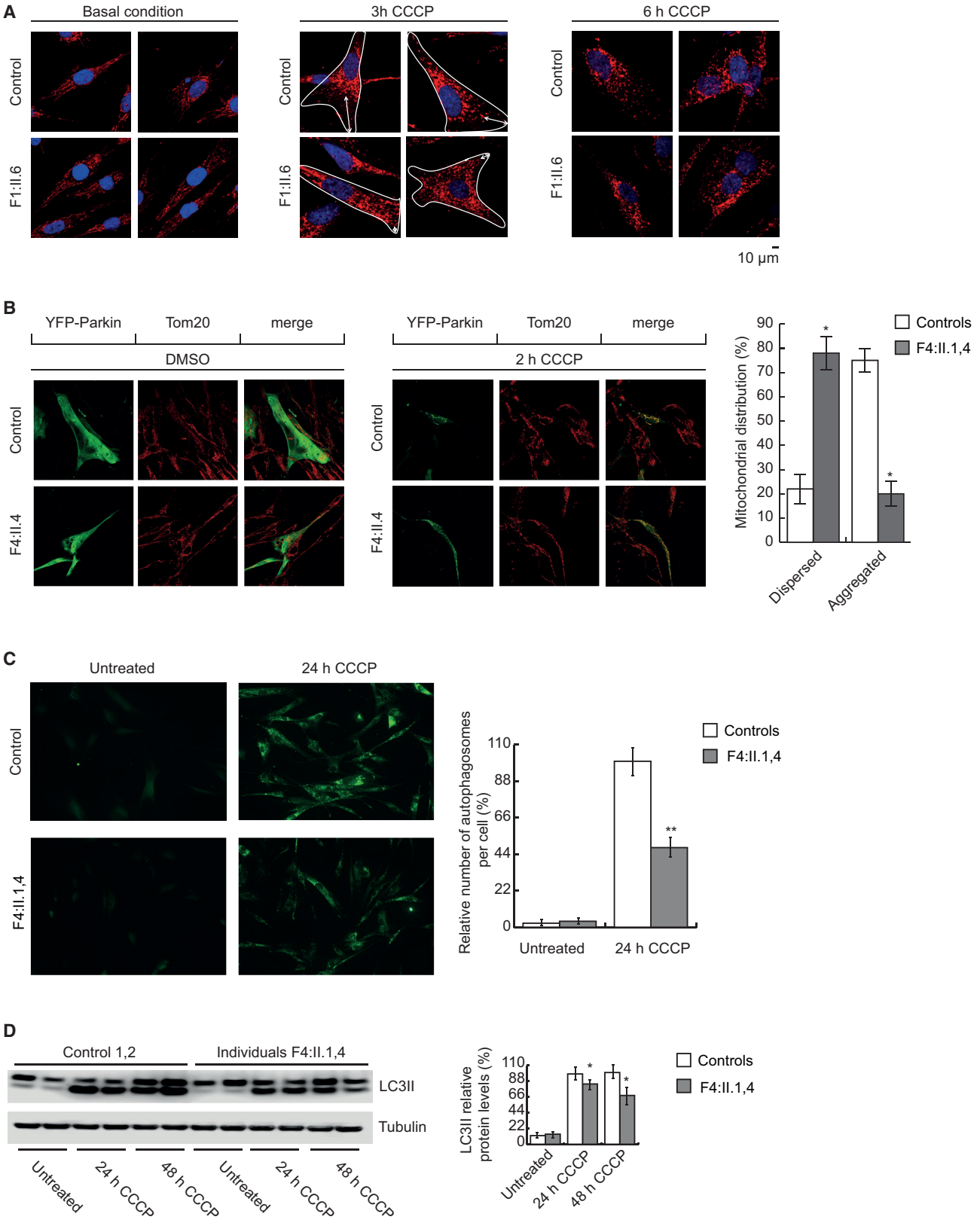

Figure 4. Investigation of Aggregation of Depolarized Mitochondria and Autophagosomal Formation

(A) Naive (no exogenous PARKIN) control and SQSTM1/p62 variant fibroblasts were treated with 20 µM CCCP for 3 and 6 hr and fixed with 4% PFA. Mitochondria were immunostained with the mitochondrial SSBP and detected with a fluorescent-labeled secondary antibody (AF568, red), nuclei were stained with DAPI (blue), and images were acquired by confocal microscopy. Depolarization of mitochondria using the protonophore CCCP led to the collapse of the mitochondrial network in control and in SQSTM1/p62 variant cells.

(legend continued on next page)

Please cite this article in press as: Haack et al., Absence of the Autophagy Adaptor SQSTM1/p62 Causes Childhood-Onset Neurodegeneration with Ataxia, Dystonia, and Gaze Palsy, The American Journal of Human Genetics (2016), http://dx.doi.org/10.1016/j.ajhg.2016.06.026

seems to be indispensable for perinuclear clustering of depolarized mitochondria in a process of self-oligomerization.[3,18,19] Furthermore, TBK1-dependent phosphorylation of SQSTM1/p62 at Ser403 has been shown to promote the efficacy of autophagosomal engulfment of ubiquitinated mitochondria at an early phase of mitochondrial depolarization.[21] We therefore studied perinuclear clustering and clearance of mitochondria in naive as well as GFP-PARKIN- and YFP-PARKIN-overexpressing control and SQSTM1/p62 variant fibroblasts after depolarization of mitochondria with the protonophore carbonyl cyanide *m*-chlorophenyl hydrazine (CCCP), the established tool to study PARKIN-dependent mitophagy in cultured cells. In naive SQSTM1/p62 variant cell lines, reduced perinuclear clustering of mitochondria was detected after 3 hr CCCP treatment compared to control cells (Figure 4A). In PARKIN-overexpressing cells (transduced with GFP-PARKIN or transfected with YFP-PARKIN), depolarization of mitochondria and subsequent collapse of the mitochondrial network led to a translocation of PARKIN to the mitochondria as indicated by co-localization with mtSSBP (Figure S3) and TOM20 (Figure 4B), replicating results of a wide literature in the field.[3,18] After 2 hr of CCCP treatment, we found a clear mitochondrial clustering in control YFP-PARKIN-overexpressing cells but not in SQSTM1/p62 variant cells (Figure 4B). No perinuclear clustering of mitochondria was observed after 2 hr treatment of oligomycin and antimycin (Figure S4). Differences in perinuclear clustering were less obvious between stably overexpressing GFP-PARKIN control and SQSTM1/p62 variant fibroblasts after 3 hr of CCCP treatment (Figure S3). We observed no difference in the overall clearance of mitochondria after 24 hr CCCP treatment in all tested conditions, in line with SQSTM1/p62 being dispensable for the PARKIN-dependent disposal of depolarized mitochondria in fibroblasts (Figures S3 and S4). In agreement, we observed no difference in mitochondrial clearance in PARKIN-overexpressing cells, treated with the respiratory chain inhibitors oligomycin and antimycin after 24 hr (Figure S4) in these cells. We next investigated the autophagic flux in SQSTM1/p62-deficient and control cell lines by monitoring changes in the levels of LC3I/II upon starvation with and without addition of the lysosomal inhibitors bafilomycin or NH_4Cl. Concordant with a functional redundancy of involved autophagy adaptors, we observed no obvious differences between control and SQSTM1/p62 variant cell lines in these assays (Figures S5 and S6). Colocalization of the autophagosomal marker LC3II and YFP-PARKIN was not affected upon CCCP treatment (Figure S7). However, depolarization of mitochondria with CCCP did result in a reduced autophagosome formation in naive SQSTM1/p62-deficient cells (Figures 4C and 4D), whereas after treatment with oligomycin-antimycin, no differences were observed between SQSTM1/p62 variant and control cell lines (Figure S8). These observations suggest that in dividing cells, SQSTM1/p62 contributes to the early regulation of mitophagy including perinuclear clustering of mitochondria and autophagosome formation upon depolarization, but that it is redundant for mitochondrial removal and autophagic flux.

In mice, the knock out of *Sqstm1* leads to mature-onset obesity, leptine resistance, and impaired glucose tolerance and insulin resistance potentially mediated by disturbed regulation of adipocyte differentiation due to enhanced basal ERK activity.[22] Furthermore, the chronic absence of Sqstm1/p62 promotes mature-onset neurodegeneration with accumulation of hyperphosphorylated tau and neurofibrillary tangles in hippocampal and cortical neurons manifesting with increased anxiety, depression, and loss of short-term memory.[23] In agreement, individuals deficient of SQSTM1/p62 did present with severely increased tau and phospho-tau levels in CSF (see F4:II.1,4 clinical description in the Supplemental Data).

To our knowledge, biallelic *SQSTM1* loss-of-function mutations have not yet been reported in humans. The present study establishes absence of SQSTM1/p62 as a molecular

After 3 hr of CCCP treatment, perinuclear clustering of mitochondria can be observed in control cells, which is less evident in SQSTM1/p62 variant fibroblasts (arrows indicate distance from outer cell membrane to clustered mitochondria). No obvious differences between cell lines were observed after 6 hr of treatment.

(B) Control and SQSTM1/p62 variant fibroblasts were transfected with YFP-Parkin (Addgene #23955),[28] treated with CCCP (20 μM) for 2 hr, followed by 4% PFA fixation. Mitochondria were immunostained using antibodies against the mitochondrial protein TOM20 (Santa Cruz cat# sc-11414, RRID: AB_793274) and detected with a fluorescent-labeled secondary antibody (AF568, red). Images were acquired by confocal microscopy. Depolarization of mitochondria using the protonophore CCCP led to the collapse of the mitochondrial network in control and in SQSTM1/p62 variant cells. After 2 hr, mitochondrial clustering can be observed in control cells, with reduced clustering in SQSTM1/p62-deficient cells. Right panel: quantification of percent of cells showing a dispersed or aggregated mitochondrial distribution after 2 hr of CCCP treatment. n = 3, 25 cells per experiment. Morphology classification was done according to previous reports studying the function of p62/SQSTM1 in mitophagy.

(C) SQSTM1/p62 variant and control cell lines were treated for 24 hr with the protonophore CCCP (20 μM) and fixed with 4% PFA. Autophagosomes were immunostained, using antibodies against the autophagosomal protein LC3II (MBL International cat# M152-3, RRID: AB_1279144) and detected with a fluorescent-labeled secondary antibody (AF488, green). Images were acquired by fluorescence microscopy and autophagosomes were counted manually. Right panel: quantification of the relative number of autophagosomes in the cell. Treatment with CCCP resulted in reduced autophagosome formation in SQSTM1-deficient cells. n = 3, 150 cells per experiment.

(D) SQSTM1/p62 variant and control cell lines were treated for 24 and 48 hr with the protonophore CCCP (20 μM). Treatment with CCCP resulted in reduced LC3II levels formation in SQSTM1/p62-deficient cells. Right panel: quantification of the relative LC3II protein levels using ImageJ software.

In (B)–(D), *$p \leq 0.05$; **$p \leq 0.01$; two-tailed unpaired t test. Error bars indicate ± SEM from the mean of three replicates.

defect underlying a childhood- or adolescence-onset neurodegenerative disorder. The pivotal features of the affected individuals' phenotypes were gait abnormalities (9/9), ataxia mostly of the upper limbs (9/9), dysarthria (9/9), dystonia (7/9), vertical gaze palsy (7/9), and mild cognitive decline (7/9). The course was remarkably similar in all nine affected individuals with onset between age 7 to 15 years and relatively slow progression. Brain MRI showed cerebellar atrophy in four out of eight individuals and signal abnormalities in basal ganglia with iron accumulation in two out of eight individuals. Of note, extensive brain iron deposition in the basal ganglia and substantia nigra is a characteristic phenotypic feature of a clinically and genetically heterogeneous group of neurodegenerative disorders subsumed under the umbrella term NBIA (neurodegeneration with brain iron accumulation).[24] Although the exact pathomechanisms leading to neurodegeneration is unknown in most of the major NBIA forms, the identification of X chromosome *WDR45* (MIM: 300526) mutations in individuals with BPAN (NBIA 5 [MIM: 300894]) suggested defective autophagy as a key pathomechanism.[25] Screening of a large cohort of 250 idiopathic NBIA individuals for *SQSTM1* variants failed to detect clinically relevant biallelic variants, indicating that brain iron accumulation is probably an inconsistent feature in SQSTM1-associated neurodegeneration. Of note, also in the PLA2G6 (MIM: 603604)-associated NBIA subtype PLAN (MIM: 610217), brain iron accumulation may be absent or subtle early in the disease course.[24]

Given the role of SQSTM1/p62 as a key player in a variety of vital cellular processes, it was unexpected that its absence is compatible with survival above age 40 years and that affected individuals display such a circumscribed neurological phenotype. This observation together with the findings in mice argues for a redundancy of involved factors and pathways or effective compensatory mechanisms to maintain cellular homeostasis. Our data indicate that SQSTM1/p62 functions are of particular importance in the brain, where the postmitotic nature of neurons poses especial challenges to the removing of damaged organelles and misfolded proteins.

In humans, heterozygous missense and truncating *SQSTM1* variants have been associated with the progressive skeletal disorder Paget disease of the bone (PDB), the neurodegenerative disorders ALS and FTD,[4] and recently distal myopathy with rimmed vacuoles.[5] Furthermore, 5q copy number gains comprising *SQSTM1* have been associated with kidney cancer.[26] Although several disease alleles are common to both PDB and ALS/FTD, others have been proposed to be ALS/FTD specific.[4] Surprisingly, heterozygous carriers of *SQSTM1* variants in our families showed no skeletal defects or neurological disease. In keeping with this, a recent large exome-sequencing study of 2,869 ALS-affected case subjects and 6,405 control subjects, which confidently implicated *TBK1* (MIM: 604834) and *OPTN* (MIM: 602432) in ALS, failed to establish a significant enrichment of rare *SQSTM1* variants relative to control subjects.[27] Therefore, despite *SQSTM1* being a promising ALS candidate gene from a cell biological perspective, additional statistical and mechanistic evidence is needed for the implication of hypomorphic alleles, putatively dominant-acting variants, or *SQSTM1* haploinsufficiency in neurodegeneration. The puzzling variety of diseases and inheritance patterns associated with *SQSTM1* variants suggests complex genotype/phenotype relationships and points to the possibility of currently unidentified modifying genes and gene-environment interactions.

Supplemental Data

Supplemental Data include clinical descriptions, seven figures, and one table and can be found with this article online at http://dx.doi.org/10.1016/j.ajhg.2016.06.026.

Acknowledgments

We thank all the families for their participation and Dr. Boriana Büchner, Dr. Ivan Karin, and Dr. Benedikt Schoser for their support in phenotyping. This study was supported by the German Bundesministerium für Bildung und Forschung (BMBF) through the German Network for Mitochondrial Disorders (mitoNET; 01GM1113A-E to T.M., H.P., and T.K.), the E-Rare project GENOMIT (01GM1207 to T.M. and H.P.), the Juniorverbund in der Systemmedizin "mitOmics" (FKZ 01ZX1405C to T.B.H.), as well as the European Commission 7th Framework Programme (FP7/2007-2013, HEALTH-F2-2011, grant agreement No. 277984, TIRCON). E.I. was supported by the Arvo and Lea Ylppö Foundation, P.I. by Foundation for Pediatric Research, and C.J.C. by a Helsinki University research grant. A.S. acknowledges support of Sigrid Jusélius Foundation, Aatos and Jane Erkko Foundation, and Academy of Finland. R.H. is a Wellcome Trust Investigator (109915/Z/15/Z) and was supported by the Medical Research Council (UK) (G1000848) and the European Research Council (309548). Additional support came from The Swedish Research Council (VR521-2012-2571 to A. Wredenberg and K2014-54X-20642-13-3 to A. Wedell), Stockholm County Council (K0176-2012 to A. Wredenberg and 20140053 to A. Wedell), Swedish Foundation for Strategic Research (ICA 12-0017 to A. Wredenberg), Knut & Alice Wallenberg Foundation (KAW 20130026 to A. Wredenberg and A. Wedell), and The Swedish Brain Foundation (FO2015-0146). A. Wredenberg is a Ragnar Söderberg fellow (M77/13). We acknowledge the "Cell Lines and DNA Bank of Paediatric Movement Disorders and Neurodegenerative Diseases" of the Telethon Network of Genetic Biobanks (grant GTB12001J) and the Eurobiobank Network. This work was supported by the Deutsche Forschungsgemeinschaft (German Research Foundation) within the framework of the Munich Cluster for Systems Neurology (EXC 1010 SyNergy) to T.M. and T.K.

Received: May 17, 2016
Accepted: June 27, 2016
Published: August 18, 2016

Web Resources

CADD, http://cadd.gs.washington.edu/
ExAC Browser, http://exac.broadinstitute.org/

OMIM, http://www.omim.org/
RRID, https://scicrunch.org/resources

References

1. Manford, A.G., and Rape, M. (2015). Better safe than sorry: interlinked feedback loops for robust mitophagy. Mol. Cell *60*, 1–2.
2. Pickrell, A.M., and Youle, R.J. (2015). The roles of PINK1, parkin, and mitochondrial fidelity in Parkinson's disease. Neuron *85*, 257–273.
3. Lazarou, M., Sliter, D.A., Kane, L.A., Sarraf, S.A., Wang, C., Burman, J.L., Sideris, D.P., Fogel, A.I., and Youle, R.J. (2015). The ubiquitin kinase PINK1 recruits autophagy receptors to induce mitophagy. Nature *524*, 309–314.
4. Rea, S.L., Majcher, V., Searle, M.S., and Layfield, R. (2014). SQSTM1 mutations–bridging Paget disease of bone and ALS/FTLD. Exp. Cell Res. *325*, 27–37.
5. Bucelli, R.C., Arhzaouy, K., Pestronk, A., Pittman, S.K., Rojas, L., Sue, C.M., Evilä, A., Hackman, P., Udd, B., Harms, M.B., and Weihl, C.C. (2015). SQSTM1 splice site mutation in distal myopathy with rimmed vacuoles. Neurology *85*, 665–674.
6. Haack, T.B., Hogarth, P., Kruer, M.C., Gregory, A., Wieland, T., Schwarzmayr, T., Graf, E., Sanford, L., Meyer, E., Kara, E., et al. (2012). Exome sequencing reveals de novo WDR45 mutations causing a phenotypically distinct, X-linked dominant form of NBIA. Am. J. Hum. Genet. *91*, 1144–1149.
7. Kremer, L.S., Distelmaier, F., Alhaddad, B., Hempel, M., Iuso, A., Küpper, C., Mühlhausen, C., Kovacs-Nagy, R., Satanovskij, R., Graf, E., et al. (2016). Bi-allelic truncating mutations in TANGO2 cause infancy-onset recurrent metabolic crises with encephalocardiomyopathy. Am. J. Hum. Genet. *98*, 358–362.
8. Plagnol, V., Curtis, J., Epstein, M., Mok, K.Y., Stebbings, E., Grigoriadou, S., Wood, N.W., Hambleton, S., Burns, S.O., Thrasher, A.J., et al. (2012). A robust model for read count data in exome sequencing experiments and implications for copy number variant calling. Bioinformatics *28*, 2747–2754.
9. Sulonen, A.M., Ellonen, P., Almusa, H., Lepistö, M., Eldfors, S., Hannula, S., Miettinen, T., Tyynismaa, H., Salo, P., Heckman, C., et al. (2011). Comparison of solution-based exome capture methods for next generation sequencing. Genome Biol. *12*, R94.
10. Kircher, M., Witten, D.M., Jain, P., O'Roak, B.J., Cooper, G.M., and Shendure, J. (2014). A general framework for estimating the relative pathogenicity of human genetic variants. Nat. Genet. *46*, 310–315.
11. Stranneheim, H., Engvall, M., Naess, K., Lesko, N., Larsson, P., Dahlberg, M., Andeer, R., Wredenberg, A., Freyer, C., Barbaro, M., et al. (2014). Rapid pulsed whole genome sequencing for comprehensive acute diagnostics of inborn errors of metabolism. BMC Genomics *15*, 1090.
12. Puls, A., Schmidt, S., Grawe, F., and Stabel, S. (1997). Interaction of protein kinase C zeta with ZIP, a novel protein kinase C-binding protein. Proc. Natl. Acad. Sci. USA *94*, 6191–6196.
13. Sanchez, P., De Carcer, G., Sandoval, I.V., Moscat, J., and Diaz-Meco, M.T. (1998). Localization of atypical protein kinase C isoforms into lysosome-targeted endosomes through interaction with p62. Mol. Cell. Biol. *18*, 3069–3080.
14. Katsuragi, Y., Ichimura, Y., and Komatsu, M. (2015). p62/SQSTM1 functions as a signaling hub and an autophagy adaptor. FEBS J. *282*, 4672–4678.
15. Moscat, J., and Diaz-Meco, M.T. (2009). p62 at the crossroads of autophagy, apoptosis, and cancer. Cell *137*, 1001–1004.
16. Bjørkøy, G., Lamark, T., Brech, A., Outzen, H., Perander, M., Overvatn, A., Stenmark, H., and Johansen, T. (2005). p62/SQSTM1 forms protein aggregates degraded by autophagy and has a protective effect on huntingtin-induced cell death. J. Cell Biol. *171*, 603–614.
17. Geisler, S., Holmström, K.M., Skujat, D., Fiesel, F.C., Rothfuss, O.C., Kahle, P.J., and Springer, W. (2010). PINK1/Parkin-mediated mitophagy is dependent on VDAC1 and p62/SQSTM1. Nat. Cell Biol. *12*, 119–131.
18. Narendra, D., Kane, L.A., Hauser, D.N., Fearnley, I.M., and Youle, R.J. (2010). p62/SQSTM1 is required for Parkin-induced mitochondrial clustering but not mitophagy; VDAC1 is dispensable for both. Autophagy *6*, 1090–1106.
19. Okatsu, K., Saisho, K., Shimanuki, M., Nakada, K., Shitara, H., Sou, Y.S., Kimura, M., Sato, S., Hattori, N., Komatsu, M., et al. (2010). p62/SQSTM1 cooperates with Parkin for perinuclear clustering of depolarized mitochondria. Genes Cells *15*, 887–900.
20. Rogov, V., Dötsch, V., Johansen, T., and Kirkin, V. (2014). Interactions between autophagy receptors and ubiquitin-like proteins form the molecular basis for selective autophagy. Mol. Cell *53*, 167–178.
21. Matsumoto, G., Shimogori, T., Hattori, N., and Nukina, N. (2015). TBK1 controls autophagosomal engulfment of polyubiquitinated mitochondria through p62/SQSTM1 phosphorylation. Hum. Mol. Genet. *24*, 4429–4442.
22. Rodriguez, A., Durán, A., Selloum, M., Champy, M.F., Diez-Guerra, F.J., Flores, J.M., Serrano, M., Auwerx, J., Diaz-Meco, M.T., and Moscat, J. (2006). Mature-onset obesity and insulin resistance in mice deficient in the signaling adapter p62. Cell Metab. *3*, 211–222.
23. Ramesh Babu, J., Lamar Seibenhener, M., Peng, J., Strom, A.L., Kemppainen, R., Cox, N., Zhu, H., Wooten, M.C., Diaz-Meco, M.T., Moscat, J., and Wooten, M.W. (2008). Genetic inactivation of p62 leads to accumulation of hyperphosphorylated tau and neurodegeneration. J. Neurochem. *106*, 107–120.
24. Hogarth, P. (2015). Neurodegeneration with brain iron accumulation: diagnosis and management. J. Mov. Disord. *8*, 1–13.
25. Saitsu, H., Nishimura, T., Muramatsu, K., Kodera, H., Kumada, S., Sugai, K., Kasai-Yoshida, E., Sawaura, N., Nishida, H., Hoshino, A., et al. (2013). De novo mutations in the autophagy gene WDR45 cause static encephalopathy of childhood with neurodegeneration in adulthood. Nat. Genet. *45*, 445–449, e1.
26. Li, L., Shen, C., Nakamura, E., Ando, K., Signoretti, S., Beroukhim, R., Cowley, G.S., Lizotte, P., Liberzon, E., Bair, S., et al. (2013). SQSTM1 is a pathogenic target of 5q copy number gains in kidney cancer. Cancer Cell *24*, 738–750.
27. Cirulli, E.T., Lasseigne, B.N., Petrovski, S., Sapp, P.C., Dion, P.A., Leblond, C.S., Couthouis, J., Lu, Y.F., Wang, Q., Krueger, B.J., et al.; FALS Sequencing Consortium (2015). Exome sequencing in amyotrophic lateral sclerosis identifies risk genes and pathways. Science *347*, 1436–1441.
28. Narendra, D., Tanaka, A., Suen, D.F., and Youle, R.J. (2008). Parkin is recruited selectively to impaired mitochondria and promotes their autophagy. J. Cell Biol. *183*, 795–803.

The American Journal of Human Genetics, Volume *99*

Supplemental Data

Absence of the Autophagy Adaptor SQSTM1/p62 Causes Childhood-Onset Neurodegeneration with Ataxia, Dystonia, and Gaze Palsy

Tobias B. Haack, Erika Ignatius, Javier Calvo-Garrido, Arcangela Iuso, Pirjo Isohanni, Camilla Maffezzini, Tuula Lönnqvist, Anu Suomalainen, Matteo Gorza, Laura S. Kremer, Elisabeth Graf, Monika Hartig, Riccardo Berutti, Martin Paucar, Per Svenningsson, Henrik Stranneheim, Göran Brandberg, Anna Wedell, Manju A. Kurian, Susan A. Hayflick, Paola Venco, Valeria Tiranti, Tim M. Strom, Martin Dichgans, Rita Horvath, Elke Holinski-Feder, Christoph Freyer, Thomas Meitinger, Holger Prokisch, Jan Senderek, Anna Wredenberg, Christopher J. Carroll, and Thomas Klopstock

CLINICAL DESCRIPTIONS

Family 1 from Germany consists of three affected individuals, one male and two females, and three healthy siblings.

Individual F1:II.1 is the first son of healthy unrelated parents of German origin. He presented at the age of 10 years with gait problems, urinary incontinence and upper limb ataxia. His gait problems steadily worsened until he was wheelchair-bound at age 16 years. Clinical examination at age 45 years revealed severe generalized dystonia, dysdiadochokinesis of the hands, severe dysarthria, vertical gaze palsy, hyporeflexia, and a mild motor axonal neuropathy. There was no history of psychiatric symptoms, seizures, tremor or visual impairment.

Individual F1:II.3, the sister of individual F1:II.1, presented at the age of 12 years with gait problems and cognitive decline. Progressive motor decline left her wheelchair-bound at age 16 years and bed-ridden at age 36 years. Clinical examination at age 42 years showed severe generalized dystonia and parkinsonism, severe dysarthria, vertical gaze palsy, and involvement of the upper (pyramidal signs) and lower (hyporeflexia, muscle atrophy) motor neurons. Other clinical findings included dysdiadochokinesis of the hands and obesity. There was no history of psychiatric abnormalities, seizures, tremor or visual impairment. Sequential brain MRIs showed normal findings at age 25 years, hyperintense basal ganglia at age 34 years, and accumulation of iron in basal ganglia at age 39 years.

Individual F1:II.6, another sister of individual F1:II.1, presented at the age of 15 years with gait problems, urinary incontinence, and upper limb ataxia. The gait problems slowly worsened until she needed a walking frame at age 30 years and occasionally a wheelchair at age 32 years. Clinical examination at ages 24, 26 and 33 years revealed a movement disorder with mild dystonia and chorea, a cerebellar syndrome with gaze-evoked nystagmus, saccadic eye pursuit, dysmetria of the upper and lower extremities and dysdiadochokinesis of the hands, a pyramidal syndrome with increased reflexes, progressive dysarthria, and obesity (105 kg). At age 33 years there were signs of dementia and visuoconstructive impairment. There was no vertical gaze palsy or lower motor neuron involvement. There was no history of psychiatric abnormalities, seizures, tremor or visual impairment. Neurography of

bilateral motor tibial nerves, right motor peroneal nerve and bilateral sensory sural nerve was unremarkable at age 24 years. Similarly, at age 33 years, neurography of right motor median nerve and right sensory radial nerve was unremarkable, as was the electromyography of right interosseous dorsalis I and biceps brachii muscles. A muscle biopsy was unremarkable regarding morphology, histochemistry, and ultrastructure. In particular, there were no signs of mitochondrial dysfunction. Brain MRI at age 33 years showed accumulation of iron in substantia nigra and globus pallidus internus (Figure 2).

Family 2 consists of three affected sisters and nine reportedly healthy siblings and originated from the United Arab Emirates. The healthy parents were unaware of consanguinity.

Individual F2:II.2, a girl, had developed unsteadiness of gait, coordination problems and cognitive decline from the age of 10 years. Clinical examination at age 31 years revealed short and thin stature, a cerebellar syndrome with ataxic stance and gait, dysdiadochokinesis, intention tremor, dysarthria and gaze-evoked nystagmus, as well as posture dystonia, mild hearing loss and marked vertical gaze palsy. The patient was still ambulatory. There were no pyramidal signs, no signs of the lower motor neuron, no sensory signs and no indication of optic atrophy or pigmentary retinopathy. Brain MRI showed mild cerebellar atrophy affecting predominantly the superior cerebellum and vermis (Figure 2). Electroneuromyography and evoked potentials were unremarkable. Laboratory tests revealed normal results for vitamin E, alpha-fetoprotein, phytanic acid, acanthocytes, lipids, and creatine kinase. Genetic testing for *FRDA*, *APTX,* and *POLG1* did not show pathogenic variants.

Individual F2:II.3 had a very similar course as her older sister. She also developed unsteadiness of gait, coordination problems and cognitive decline from the age of 10 years on. Clinical examination at age 18 years revealed short and thin stature, marked vertical gaze palsy, a mild cerebellar syndrome, mild postural dystonia, mild hearing loss and slowed speech. Otherwise, neurological examination was unremarkable. Brain MRI showed mild cerebellar atrophy of the vermis. Electroneuromyography, evoked potentials and laboratory tests were unremarkable.

Individual F2:II.4 had a very similar course as her older sisters. She also developed unsteadiness of gait, coordination problems and cognitive decline from the age of 10 years. Clinical examination at age 12 years revealed short and thin stature, marked vertical gaze palsy, a mild cerebellar syndrome, mild hearing impairment, and a mild athetotic movement disorder. Otherwise, neurological examination was unremarkable. Brain MRI showed mild cerebellar atrophy. Electroneuromyography, evoked potentials and laboratory tests were unremarkable.

Of note, disease progression was slow in all siblings and they were still able to walk independently aged 12, 18, and 31 years, respectively.

Family 3 from Finland consists of one affected sister and one healthy brother.

Individual F3:II.1 is a 19-year-old female with normal early development. Her parents Her parents were reportedly unrelated. The mother had hypothyroidism; otherwise the family members were healthy. At the age of 7 years, she had varicella infection with high fever and severe skin blisters. Two months after the infection she presented with tremor, oculomotor apraxia and dysarthria. She developed ataxia and myoclonic jerks. Her cognitive performance declined after the onset of the symptoms. At the last investigation at the age of 18 years the clinical examination showed broad-based gait, accelerated but not clonic deep tendon reflexes, and negative Babinski sign. The tremor had improved. She walked with a wide based gait. Her deep tendon reflexes were accelerated, but not clonic, and the Babinski sign was negative. After the varicella infection, hypothyroidism was diagnosed and treated with levothyroxine. Transaminases were elevated up to three-fold during infections. Her BMI at the age of 18 years was 15.6, with a height of 162 cm and weight of 41 kg. There was no history of psychiatric symptoms, seizures, or visual impairment. Muscle biopsy performed at the age of 18 years was unremarkable regarding morphology, histochemistry, and ultrastructure. Respiratory chain enzyme analysis was normal, except for a slight decrease in complex IV activity. EEG showed 3 Hz spikes during sleep at the age of 9, control EEGs at the ages of 13 and 18 years were normal. Electroneuromyography has been performed twice at the age of 13 and 18 years with normal results. Multiple laboratory studies have been performed and remained normal; including urine catecholamines, organic acids, and amino

acids, serum concentrations of vitamin E, copper, ceruloplasmin, creatine kinase, very long chained fatty acids, phytanic acid, and lactate. Common pathogenic variants of *PME* and *POLG1* were excluded. Brain MRI was normal at the age of 7 and 13 years, but mild to moderate cerebellar upper vermian atrophy was seen at the age of 18 years (Figure 2).

Family 4 consists of two affected individuals, one male and one female, and two healthy siblings. The family originates from Syria and are of Kurdish descent. The healthy parents are cousins.

F4:II.1 is the first daughter and presented with ataxia and urinary incontinence at 8 years of age. The symptoms progressed and she additionally developed vertical gaze palsy, gaze-evoked nystagmus in all directions, dysarthria and slowed speech, as well as muscle weakness in the upper body with atrophy of thenar muscles and scoliosis. She has cognitive impairment and never learnt to read. Other clinical findings included dysdiadochokinesis, reduced postural control, and dysmetria of the hands. At age 33 years she is walking with a broad-based gait and now needs aid. She has no history of psychiatric symptoms, pyramidal or sensory signs, seizures or tremor. Her symptoms have not progressed over the past five years. Brain MRI, EEG and EMG showed normal findings. Very long chain fatty acids, sialic acids in urine, and CDT levels were normal. Analysis of cerebrospinal fluid showed increased levels of beta-amyloid 950 ng/L (<550), phospho-tau 200 ng/L (<60) and tau protein >1200 ng/L (<300). Investigation of mitochondrial histology and electron microscopy from a muscle biopsy showed normal findings at the age of 31 years. Sanger sequencing was performed on the complete mtDNA isolated from muscle and *FRDA, ATXN*, and *CACNA1A* from DNA isolated from blood, without positive findings.

Individual F4:II.4 had a similar course as his older sister, although he is more severely affected regarding motor functions, but cognitively less impaired and reads properly. He developed ataxia, vertical gaze palsy, and gaze-evoked nystagmus at 8 years of age. The symptoms progressed and he also developed dysarthria and slowed speech, generalized dystonia, and severely impaired gait and postural control with frequent falls. At the age of 17 years, he is now wheelchair-bound. He has mild cognitive impairment. He has no history of psychiatric symptoms, pyramidal or sensory signs, seizures or tremor. Brain MRI, EEG,

EMG, ERG and ENG showed normal findings. Very long chain fatty acids, sialic acids and oligosaccharides in urine were normal. Organic acids in urine and plasma and urine amino acids were normal. Analysis of cerebrospinal fluid showed increased levels of neurofilament light protein 420 ng/L (<250), glial fibrillar acidic protein 820ng/L (<175), beta-amyloid 1280 ng/L (<550), phospho-tau 420 ng/L (<60) and tau protein >1200 ng/L (<300). Investigation of mitochondrial histology and electron microscopy from a muscle biopsy showed normal findings at the age of 15 years. Mitochondrial ATP production rate and respiratory chain enzyme activities were towards the lower end of normal, with complex IV activity being mostly affected. In agreement with the mild complex IV defect observed in muscle biopsies from patients F3:II.1 and F4:II.4, fibroblasts grown on galactose as carbon source showed a mild complex IV defect (Figure S1). Sanger sequencing was performed on the complete mtDNA isolated from muscle and *APTX*, *FRDA, SETX, ATP13A2,* and *POLG* from DNA isolated from blood, without positive findings.

SUPPLEMENTARY FIGURES

Figure S1

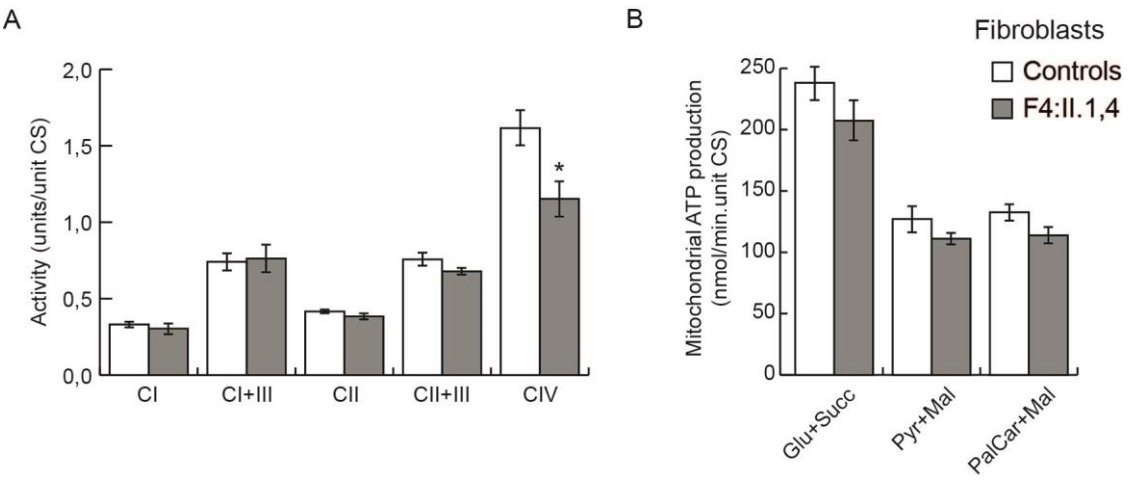

Figure S1 Mitochondrial ATP production and OXPHOS enzyme activity.
Fibroblasts were grown for 1 week in 0.9g/L galactose and dialysed FBS at 37° C in a 5 % CO_2 atmosphere. Measurement of respiratory chain activities (A) and of ATP production (B) were performed as previously described.[1] Error bars indicate ± SEM. *, $p \leq 0.05$ (two-tailed unpaired t-test.

Supplemental References

1. Wibom, R., Hagenfeldt, L., and von Dobeln, U. (2002). Measurement of ATP production and respiratory chain enzyme activities in mitochondria isolated from small muscle biopsy samples. Analytical biochemistry 311, 139-151.

Figure S2

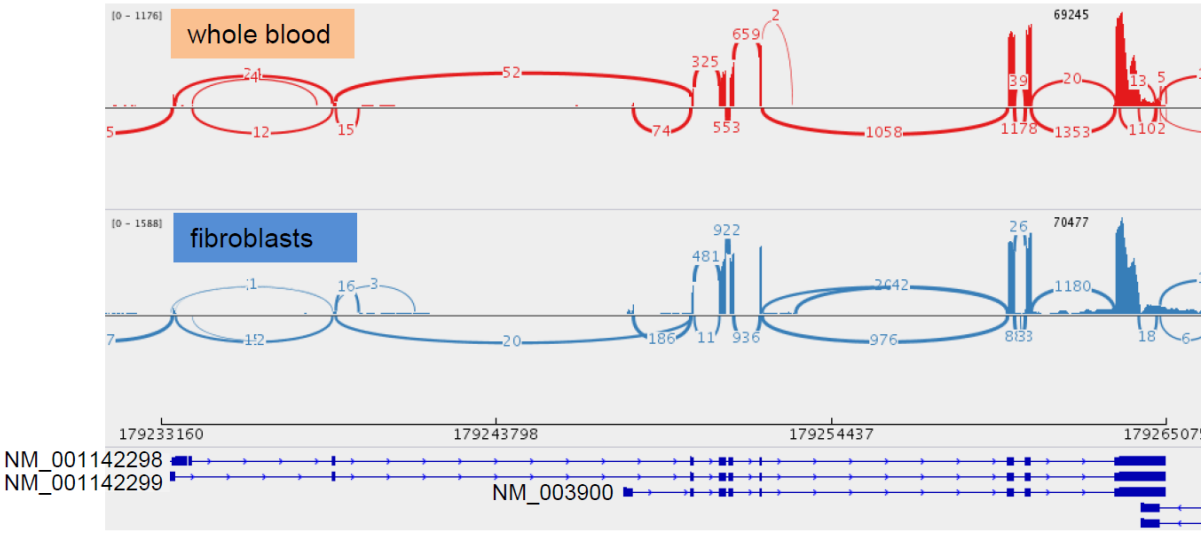

Figure S2 Sashimi plot of RNA sequences produced from whole blood (red, upper panel) and fibroblast cell lines (blue, lower panel). In whole blood, about 59 % of reads (74 out of 126) and in fibroblasts, about 90 % of reads (186 out of 206) indicate the expression of the isoform NM_003900.

Figure S3

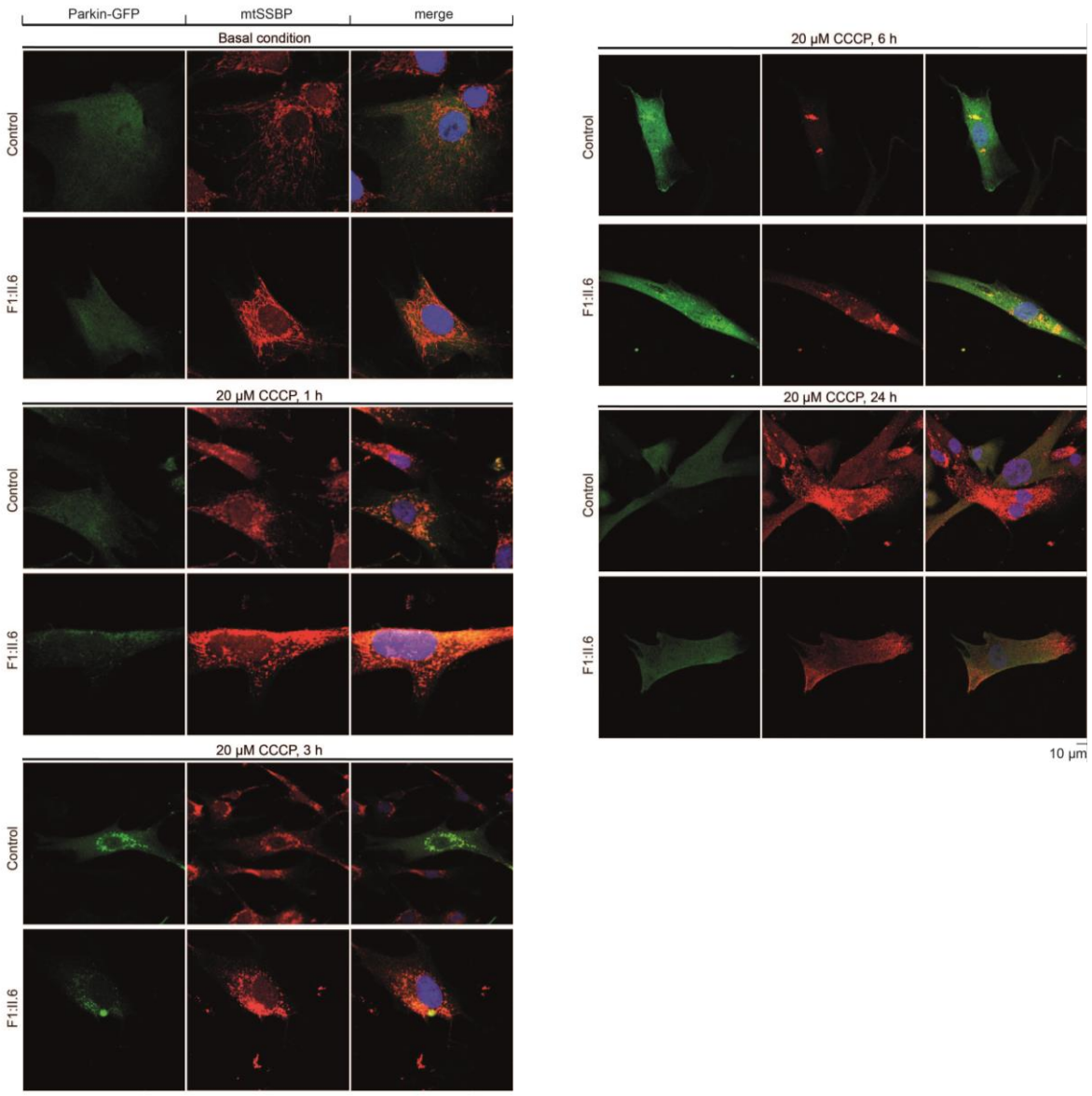

Figure S3 Control and SQSTM1-mutant fibroblasts were transduced with Parkin-GFP (green) and treated with CCCP (20 µM) for 1, 3, 6 and 24 h. Mitochondria were immunostained with the mitochondrial SSBP (mtSSBP) and detected with a secondary fluorescent-conjugated antibody (AF568, red). Nuclei were stained with DAPI (blue). Co-localization between Parkin and mitochondria were visualized among Parkin-GFP-positive cells by fluorescent confocal microscopy. Depolarization of mitochondria using the protonophore CCCP led to translocation of Parkin-GFP from the cytosol to perinuclear mitochondria in control as well as in SQSTM1-mutant cells. Coincident with Parkin translocation, mitochondrial networks in CCCP-treated cells collapsed around the perinuclear region, as revealed by mtSSBP. Both in control cells and in SQSTM1 variant cells, Parkin translocation to mitochondria was followed, within 24 hours, by almost complete loss of the mitochondrial marker mtSSBP, and back diffusion of Parkin into the cytosol.

Figure S4

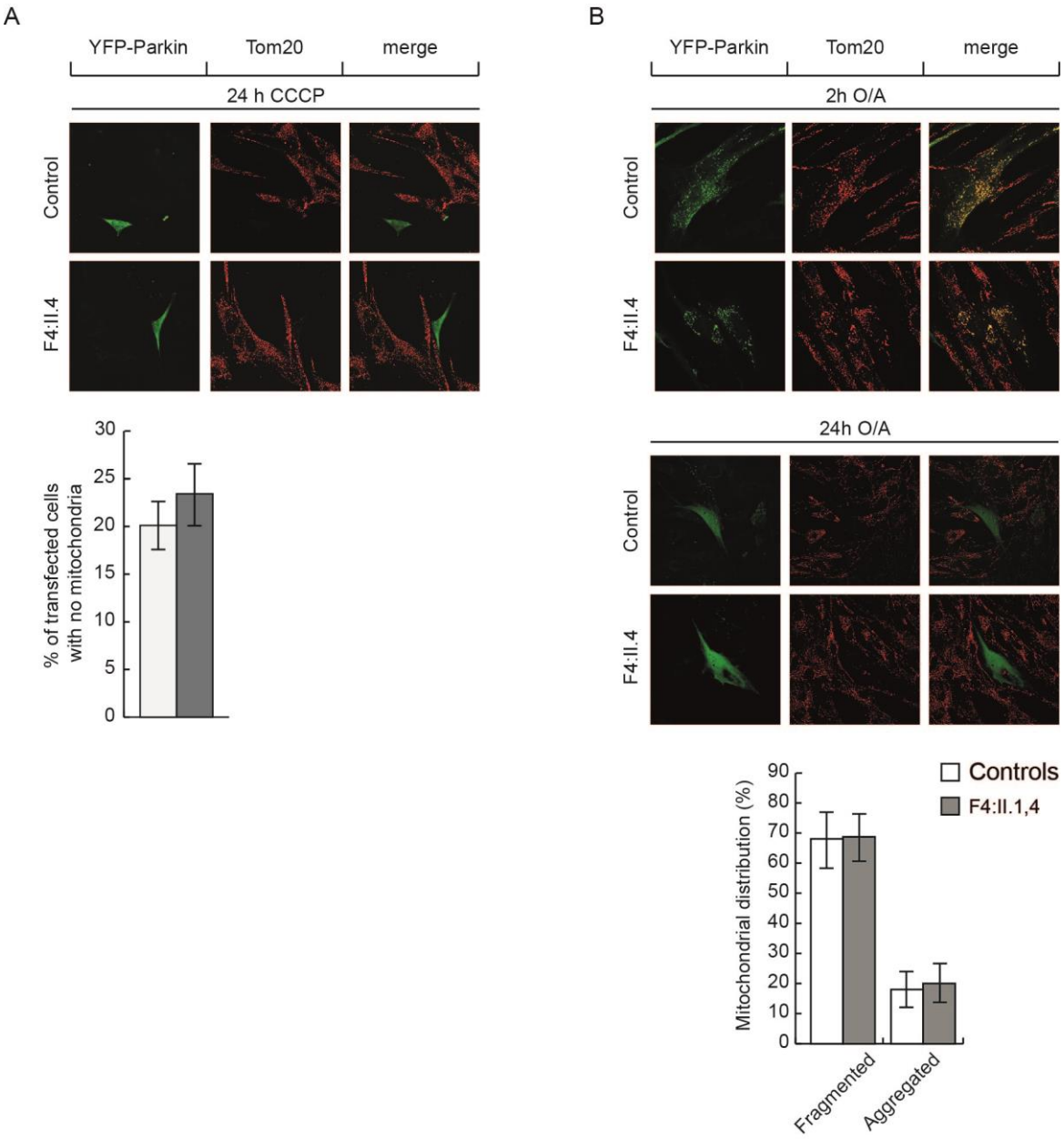

Figure S4 Investigation of Aggregation and Clearance of Depolarized Mitochondria after CCCP and Oligomycin-Antimycin Treatment.

(A) Control and SQSTM1/p62 variant fibroblasts were transfected with YFP-Parkin (Addgene #23955), treated with CCCP (20 µM) for 24 h, followed by 4 % PFA fixation. Mitochondria were immunostained using antibodies against the mitochondrial protein TOM20 (sc-11414, Santa Cruz) and detected with a fluorescent-labelled secondary antibody (AF568, red). Images were acquired by confocal microscopy. Parkin translocation to mitochondria was observed within 24h, followed by an almost complete loss of the mitochondrial marker TOM20, and diffusion of Parkin within the cytosol. Quantification of % of cells showing no mitochondrial staining after 24 h of CCCP treatment.

(B) Control and SQSTM1/p62 variant fibroblasts were transfected with YFP-Parkin (green), treated with oligomycin (10 µM) and antimycin (1 µM) for 2 and 24 h and fixed with 4 % PFA. Mitochondria were immunostained using antibodies against the mitochondrial protein Tom20, and detected with a fluorescent-labelled secondary antibody (AF568, red). Images were acquired by confocal microscopy. Depolarization of mitochondria using oligomycin-antimycin led to the collapse of the mitochondrial network already after 2 h of treatment, both in control and in SQSTM1-mutant cells. Parkin translocation to mitochondria was observed within 24h, followed by an almost complete loss of the mitochondrial marker TOM20, and diffusion of

Parkin within the cytosol. Quantification of % of cells showing a dispersed or aggregated mitochondrial distribution after 2 h of oligomycin-antimycin treatment.

Figure S5

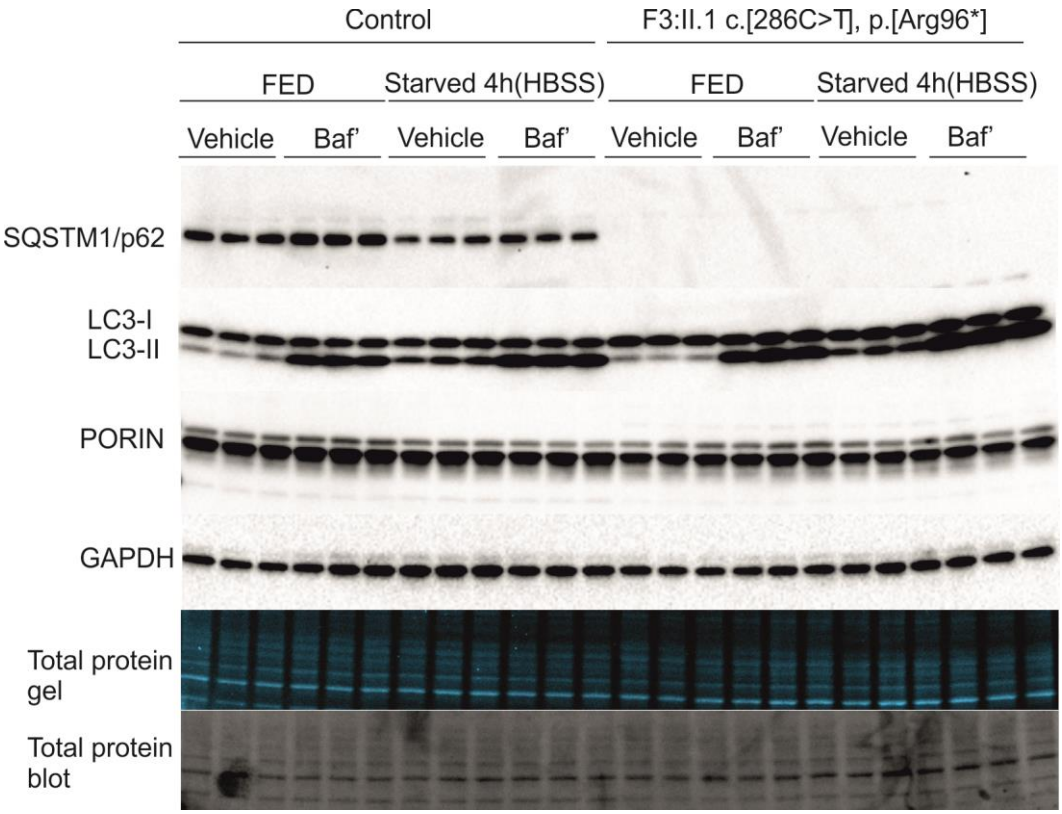

Figure S5 Investigation of Autophagic Flux.
Investigation of autophagic flux in SQSTM1/p62 variant and control cell lines upon starvation with and without addition of the lysosomal inhibitor bafilomycin (baf') at a concentration of 100 nM. Cells were starved for 4 h by incubation in HBSS and autophagy flux determined by accumulation of LC3II measured in immunoblot. Accumulation of LC3II was similar in both control and SQSTM1/p62 variant cells indicating starvation induced autophagy proceeds normally in absence of SQSTM1/p62. Protein loading is indicated by immunoblotting with antibodies for PORIN and GAPDH, and stainfree technology (Biorad) indicates protein loading (total protein gel) and transfer (total protein blot).

Figure S6

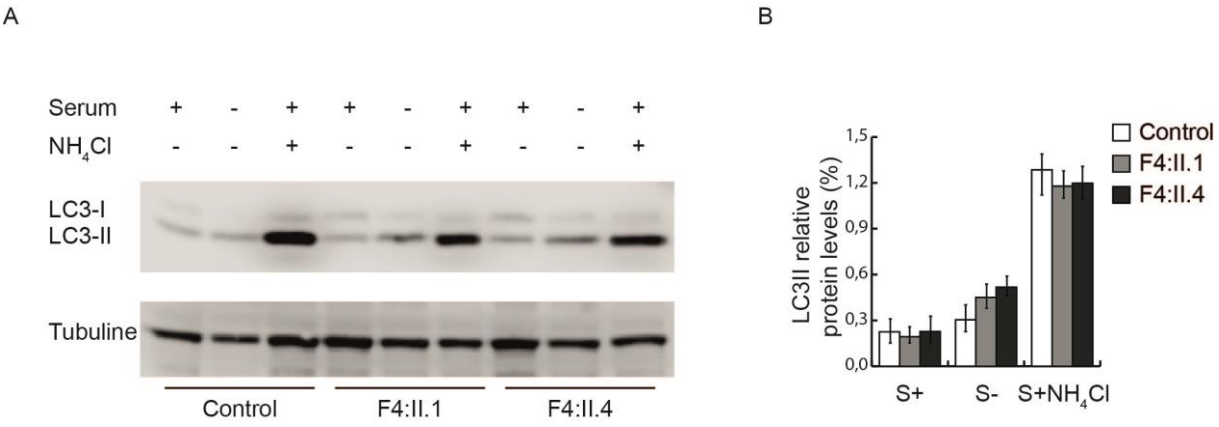

Figure S6 Investigation of Autophagic Flux.
(A) SQSTM1/p62 variant and control cell lines upon starvation for 4 h with and without addition of the lysosomal inhibitor NH4Cl (20 µM) for 2 h. Cells were harvested and lysed in RIPA buffer, followed by SDS-PAGE and Western blotting. Membranes were immunoblotted with antibodies against LC3II (L8918, Sigma) and tubulin (T6199, Sigma).
(B) Quantification of LC3II relative protein levels.

Figure S7

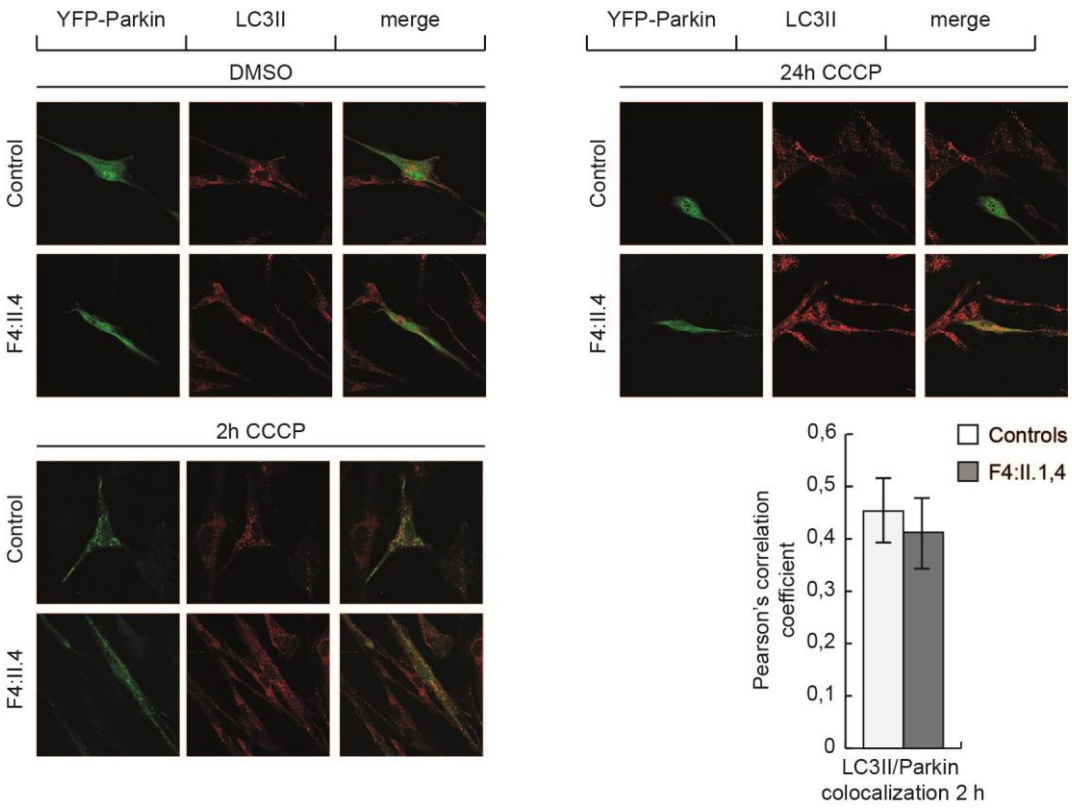

Figure S7 Investigation of LC3-Parkin Colocalization.
Control and SQSTM1/p62 variant fibroblasts were transfected with Parkin-YFP (green), treated with CCCP (20 µM) for 2 and 24 h and fixed with 4 % PFA. Autophagosomes were immunostained using antibodies against the autophagosomal protein LC3II (M152-3, MBL) and detected with a fluorescent-labelled secondary antibody (AF568, red). Images were acquired by confocal microscopy. Pearson's correlation coefficient of the colocalization between the autophagosomal marker LC3II and YFP-Parkin after 2 h of CCCP treatment.

Figure S8

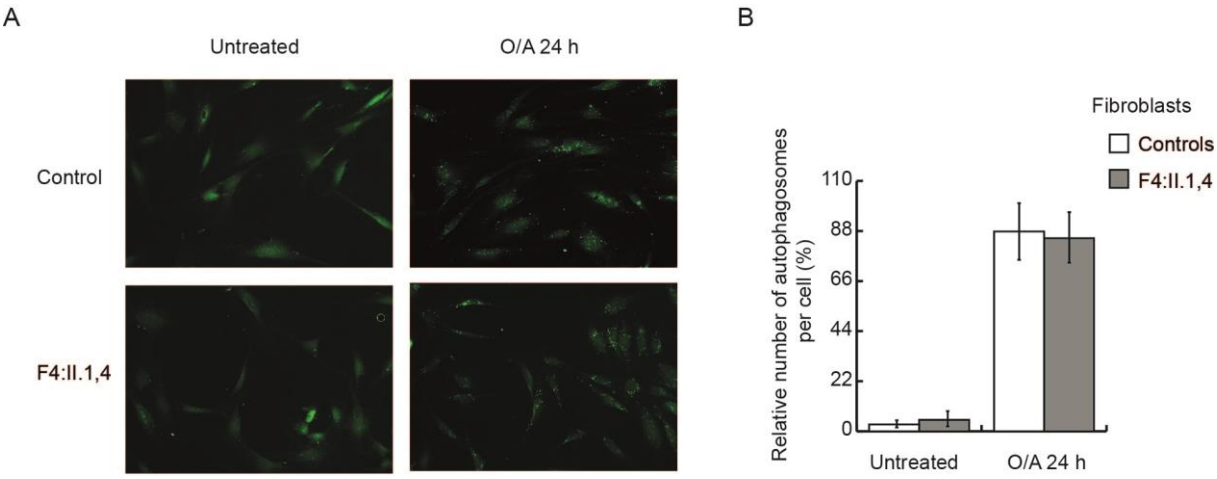

Figure S8 Investigation of Autophagosome Formation Upon Oligomycin-Antimycin Treatment.
(A) SQSTM1/p62 variant and control cell lines were treated for 24 h with oligomycin (10 µM) antimycin (1 µM) and fixed with 4 % PFA. Autophagosomes were immunostained using antibodies against the autophagosomal protein LC3II and detected with a fluorescent-labelled secondary antibody (AF488, green). Images were acquired by fluorescence microscopy.
(B) Quantification of the relative number of autophagosomes in the cell after oligomycin-antimycin treatment. No differences were found between SQSTM1/p62 variant and control cell lines.

SUPPLEMENTARY TABLE

Table S1. Variants Prioritized by Exome Sequencing in Four Families

Family 1

Individual F1:II.6											Individual F1:II.1		Individual F1:II.3	
n	Chr (hg 19)	Gene	Omim	Function	pph2	pph2 prob	Sift	CADD	Variant alleles	Transcripts	Position covered > 10x	Detected	Position covered > 10x	Detected
1	chr1:109792736-109792745	*CELSR2*		indel					homozygous	uc001dxa.4,CELSR2,+,34_35insCGC,1,indel,109792735,+CGC,del:	low coverage	No (IGV)	low coverage	No (IGV)
2	chr1:45797890-45797890	*MUTYH*	604933	missense,intronic	benign	0.001 0.002	0.24	20.6	heterozygous	uc001cnf.3,MUTYH,-,797C->T,1,non-syn,Arg266His: uc009vxo.3,MUTYH,-,797C->T,1,non-syn,Arg266His: uc001cng.3,MUTYH,-,830C->T,1,non-syn,Arg277His: uc001cnj.3,MUTYH,-,521C->T,1,non-syn,Arg174His: uc001cni.3,MUTYH,-,797C->T,1,non-syn,Arg266His: uc001cnh.3,MUTYH,-,800C->T,1,non-syn,Arg267His: uc001cnm.3,MUTYH,-,872C->T,1,non-syn,Arg291His: uc001cno.3,MUTYH,-,521C->T,1,non-syn,Arg174His: uc001cnl.3,MUTYH,-,839C->T,1,non-syn,Arg280His: uc009vxp.3,MUTYH,-,881C->T,1,non-syn,Arg294His: uc001cnn.3,MUTYH,-,842C->T,1,non-syn,Arg281His: uc010oil.2,MUTYH,-,intronic:	Yes	Yes	Yes	No
	chr1:45805964-45805966			indel,5utr,noncoding, regulation					heterozygous	uc009vxq.3,TOE1,+,40_42delGCA,0,del_1aa,Ala: uc010oim.2,TOE1,+,40_42delGCA,0,del_1aa,Ala: uc010oln.1,TOE1,+,40_42delGCA,0,del_1aa,Ala: uc001cnr.4,TOE1,+,noncoding: uc001cnm.3,MUTYH,-,5utr: uc001cno.3,MUTYH,-,5utr: uc010oil.2,MUTYH,-,5utr: uc001cnl.3,MUTYH,-,5utr: uc009vxp.3,MUTYH,-,5utr: uc001cnn.3,MUTYH,-,5utr:	Yes	Yes	Yes	No
3	chr20:55099974-55099974	*GCNT7*		missense,intronic	benign	0	1	0.004	homozygous	uc002xxx.3,FAM209A,+,110A->C,1,non-syn,Gln37Pro: uc010zzh.3,FAM209B,+,110A->C,1,non-syn,Gln37Pro: uc010zzg.1,GCNT7,-,intronic:	Yes	No	Yes	Yes
	chr20:55099977-55099977			missense,intronic	benign	0	1	0.003	homozygous	uc002xxx.3,FAM209A,+,113A->G,1,non-syn,Tyr38Cys: uc010zzh.3,FAM209B,+,113A->G,1,non-syn,Tyr38Cys: uc010zzg.1,GCNT7,-,intronic:	Yes	No	Yes	Yes
4	chr20:62190630-62190630	*HELZ2*		missense	benign	0.145 0.069	1	22.7	heterozygous	uc002yfl.1,HELZ2,-,6212C->A,1,non-syn,Arg2071Leu: uc002yfm.2,HELZ2,-,7919C->A,1,non-syn,Arg2640Leu:	Yes	No	Yes	No
	chr20:62194612-62194612			nonsense			0.78	35	heterozygous	uc002yfl.1,HELZ2,-,3856G->A,0,non-syn,Gln1286Stop: uc002yfm.2,HELZ2,-,5563G->A,0,non-syn,Gln1855Stop:	low coverage	No (IGV)	low coverage	No (IGV)
5	**chr20:55099974-55099974**	***SQSTM1***	**601530**	**missense,intronic ,regulation**	**benign**	**0.168 0.083**	**0**	**24.9**	**homozygous**	**uc003mkw.4,SQSTM1,+,2T->A,1,non-syn,Met1Lys: uc011dgr.2,SQSTM1,+,intronic: uc011dgs.2,SQSTM1,+,intronic:**	**No**	**- (Sanger confirmed)**	**No**	**- (Sanger confirmed)**
6	chr5:180631627-180631627	*TRIM7*		missense,regulation	benign	0.019 0.107	0.81	13.06	homozygous	uc003mna.2,TRIM7,-,484C->A,0,non-syn,Ala162Ser: uc003mnz.1,TRIM7,-,484C->A,0,non-syn,Ala162Ser:	No	-	No	-
7	chr9:139354517-139354517	*SEC16A*		missense	probably damaging	1	0.01	34	heterozygous	uc004chv.4,SEC16A,-,3220C->T,0,non-syn,Gly1074Arg: uc004chw.3,SEC16A,-,5050C->T,0,non-syn,Gly1684Arg: uc004chx.3,SEC16A,-,5050C->T,0,non-syn,Gly1684Arg: uc010nbn.3,SEC16A,-,5050C->T,0,non-syn,Gly1684Arg:	No	-	No	-
	chr9:139370120-139370120			missense	benign	0.026 0.024 0.01	0.13	9.571	heterozygous	uc004chv.4,SEC16A,-,829C->T,0,non-syn,Ala277Thr: uc004chw.3,SEC16A,-,1948C->T,0,non-syn,Ala650Thr: uc004chx.3,SEC16A,-,1948C->T,0,non-syn,Ala650Thr: uc010nbo.1,SEC16A,-,1948C->T,0,non-syn,Ala650Thr: uc010nbn.3,SEC16A,-,1948C->T,0,non-syn,Ala650Thr:	No	-	No	-

Family 2

Individual F2:II.2											Comment
1	chr1:203186093-203186093	*CHIT1*	600031	missense,noncoding ,intronic	benign	0.004 0.09 0.003	0.05	22.6	heterozygous	uc009xal.2,CHIT1,-,1238G->A,1,non-syn,Ala413Val:	
	chr1:203192642-203192642			missense,noncoding	benign	0.003 0.024	0.31	11.45	heterozygous	uc009xal.2,CHIT1,-,461C->T,1,non-syn,Arg154His:	
2	chr1:36553076-36553076	*TEKT2*		missense	probably damaging	0.987	0.01	34	homozygous	uc001bzr.3,TEKT2,+,892C->T,0,non-syn,Arg298Trp:	not segregregating with disease
3	chr1:43212415-43212415	*LEPRE1*	610339	missense,3utr	benign	0.006	0.38	2.715	homozygous	uc001chv.2,LEPRE1,-,2164G->T,0,non-syn,Gln722Lys:	
4	chr2:220420903-220420903	*OBSL1*	610991	missense	probably damaging	0.999	0 0.05	28	heterozygous	uc010fw k.3,OBSL1,-,4448C->A,1,non-syn,Trp1483Leu:	
	chr2:220422194-220422194			missense,intronic	probably damaging	1	0.4	24.5	heterozygous	uc010fw k.3,OBSL1,-,3937C->T,0,non-syn,Gly1313Arg:	
5	chr2:30966306-30966306	*CAPN13*		missense,noncoding	benign	0.012	0.35	0.152	heterozygous	uc021vfm.1,CAPN13,-,176C->T,1,non-syn,Arg459Gln:	
	chr2:31010026-31010026			missense	possibly damaging	0.744	0.1	16.37	heterozygous	uc021vfm.1,CAPN13,-,166G->A,0,non-syn,Arg456Cys:	
6	chr3:49395673-49395674	*GPX1*		frameshift,regulation					homozygous	uc021w xw .1,GPX1,-,38_39insGCCGCCGCCGCCG,1,frame-shift,49395673,+GCCGCCGCCGCCG,ins:	not segregregating with disease
7	chr3:64672501-64672501	*ADAMTS9*		missense,5utr,intronic,regulation	benign	0.015 0.007	0.11	20.5	heterozygous	uc003dmg.3,ADAMTS9,-,259C->A,0,non-syn,Ala87Ser:	
	chr3:64672534-64672534			missense,5utr,intronic,regulation	benign	0.002 0.001	1	4.179	heterozygous	uc003dmg.3,ADAMTS9,-,226T->C,0,non-syn,Ile76Val:	
8	chr4:2701672-2701672	*FAM193A*		missense,noncoding	benign	0 0.001	0.74	0.003	heterozygous	uc010ick.3,FAM193A,+,3500A->G,1,non-syn,Asn1167Ser:	
	chr4:2701816-2701816			missense,noncoding	benign	0.004 0.021	0.18	19.8	heterozygous	uc010ick.3,FAM193A,+,3644A->G,1,non-syn,Lys1215Arg:	
9	chr4:70465032-70465032	*UGT2A1*		missense	probably damaging possibly damaging	0.95 0.897 0.98 0.512 0.966	0.03	28.9	heterozygous	uc010ihs.3,UGT2A2,-,823G->A,0,non-syn,Arg275Cys:	
	chr4:70504919-70504919			missense,intronic	benign	0.003 0.002	1	1.459	heterozygous	uc010ihs.3,UGT2A2,-,440C->T,1,non-syn,Arg147Lys:	
10	chr5:131325809-131325809	*ACSL6*	604443	missense,noncoding	probably damaging	0.99 1 0.978	0	34	heterozygous	uc010jdn.2,ACSL6,-,359C->A,1,non-syn,Trp120Leu:	
	chr5:131329851-131329851			missense,noncoding ,regulation	benign	0.005 0.014 0.003 0.007 0.008	0.11	23.5	heterozygous	uc010jdn.2,ACSL6,-,68C->T,1,non-syn,Arg23His:	
11	**chr5:179250865-179250866**	***SQSTM1***	**601530**	**frameshift,regulation**					**homozygous**	**uc003mkw.4,SQSTM1,+,311_312delAG,2,frame-shift,179250864,-AG,del:**	**segregating with disease**
12	chr6:161771227-161771227	*PARK2*	602544	missense,stoploss,noncoding	probably damaging	0.998 0.912 0.954	0	33	homozygous	uc003qtx.4,PARK2,-,1302C->T,2,non-syn,Met434Ile:	not segregregating with disease
13	chr7:100674464-100674464	*MUC17*		missense,noncoding	benign	0.039	0.47	0.005	heterozygous	uc003uxp.1,MUC17,+,146A->G,1,non-syn,Asn49Ser:	
	chr7:100678179-100678179			missense,noncoding	benign	0.014	0.42	7.478	heterozygous	uc003uxp.1,MUC17,+,3482C->T,1,non-syn,Pro1161Leu:	
14	chr7:141490396-141490396	*TAS2R5*		missense	possibly damaging	0.823	0.02	24.5	heterozygous	uc003vwr.1,TAS2R5,+,235C->T,0,non-syn,Arg79Cys:	
	chr7:141490499-141490499			missense	probably damaging	0.985	0.82	24.1	heterozygous	uc003vwr.1,TAS2R5,+,338C->T,1,non-syn,Pro113Leu:	
15	chr7:150942624-150942624	*SMARCD3*		missense,regulation	benign probably damaging	0.317 0.969 0.336 0.353	0.33	27.2	heterozygous	uc003w js.3,SMARCD3,-,212C->A,1,non-syn,Arg71Leu:	
	chr7:150942744-150942744			missense,regulation	benign possibly damaging	0.314 0.744 0.195 0.096	0.35	22.4	heterozygous	uc003w js.3,SMARCD3,-,92G->T,1,non-syn,Pro31Gln:	
16	chr8:17612342-17612342	*MTUS1*		missense,noncoding	benign	0.003 0.007	0.5	14.09	heterozygous	uc003w xv.3,MTUS1,-,975C->A,2,non-syn,Gln325His:	
	chr8:17612343-17612343			missense,noncoding	benign possibly damaging	0.259 0.466	0.03	23.5	heterozygous	uc003w xv.3,MTUS1,-,974T->G,1,non-syn,Gln325Pro:	
17	chr10:128193312-128193312	*C10orf90*		missense	benign	0.002 0.003 0.005 0.006	1	0.004	heterozygous	uc009yao.2,C10orf90,-,748C->T,0,non-syn,Ala250Thr:	
	chr10:128193350-128193350			missense	probably damaging	0.999 0.997	0	26.2	heterozygous	uc009yao.2,C10orf90,-,710A->G,1,non-syn,Ile237Thr:	
18	chr11:43425621-43425621	*TTC17*		missense	benign	0	0.99	1.076	homozygous	uc001mxj.3,TTC17,+,716A->G,1,non-syn,Asn239Ser:	
19	chr11:5172807-5172807	*OR52A1*		missense	possibly damaging	0.734	0	27.4	heterozygous	uc010gyy.2,OR52A1,-,793G->A,0,non-syn,His265Tyr:	
	chr11:5173408-5173408			missense	benign	0.101	0.03	19.19	heterozygous	uc010gyy.2,OR52A1,-,192G->C,2,non-syn,Phe64Leu:	
20	chr11:6007202-6007202	*OR52L1*		missense	probably damaging	0.978	0.16	18.68	heterozygous	uc001mcd.2,OR52L1,-,959C->T,1,non-syn,Arg320Gln:	
	chr11:6007352-6007352			missense	probably damaging	0.999	0.01	23.7	heterozygous	uc001mcd.2,OR52L1,-,809T->C,1,non-syn,Tyr270Cys:	
21	chr11:92507224-92507224	*FAT3*		missense	benign	0.008	0.58	18.46	heterozygous	uc001pdj.4,FAT3,+,4213G->A,0,non-syn,Ala1405Thr:	
	chr11:92577727-92577727			missense	benign	0.001 0	0.52	0.018	heterozygous	uc001pdj.4,FAT3,+,11194A->G,0,non-syn,Ile3732Val:	
22	chr16:31087950-31087950	*ZNF646*		missense,regulation	probably damaging	0.935	0.24	22.9	heterozygous	uc002eap.3,ZNF646,+,3056G->C,1,non-syn,Arg1020Pro:	
	chr16:31091757-31091757			missense	benign	0.011	0.09	11.84	heterozygous	uc002eap.3,ZNF646,+,4112G->A,1,non-syn,Arg1371His:	
23	chr16:48177876-48177876	*ABCC12*		missense,noncoding	benign	0.004 0.01	0.22	14.2	heterozygous	uc002efc.1,ABCC12,-,220C->T,0,non-syn,Val74Ile:	
	chr16:48180260-48180260			missense,noncoding	benign	0.009 0.075	0.54	17.21	heterozygous	uc002efc.1,ABCC12,-,76C->T,0,non-syn,Asp26Asn:	
24	chr17:44127974-44127974	*KANSL1*	612452	missense	benign	0.002 0.017	0.62	12.96	heterozygous	uc002ikc.3,KANSL1,-,1945G->C,0,non-syn,His649Asp:	
	chr17:44172062-44172062			missense	benign	0.281 0.13	0.02	34	heterozygous	uc002ikc.3,KANSL1,-,1295C->A,1,non-syn,Arg432Leu:	
25	chr17:80399056-80399056	*HEXDC*		syn,missense,noncoding	benign	0.004	0.02	1.289	heterozygous	uc002kev.4,HEXDC,+,1166C->T,1,non-syn,Pro389Leu:	
	chr17:80400164-80400164			syn,missense,noncoding	benign	0.104	0.09	24.6	heterozygous	uc002kev.4,HEXDC,+,1454G->A,1,non-syn,Cys485Tyr:	
	chr17:80400236-80400236			syn,missense,noncoding	benign	0.037	0	22.7	heterozygous	uc002kev.4,HEXDC,+,1526C->A,1,non-syn,Ala509Glu:	
26	chr20:34091767-34091767	*CEP250*		missense	benign	0.004	0.18	1.213	heterozygous	uc021w co.1,CEP250,+,5570G->A,1,non-syn,Arg1857His:	
	chr20:34092354-34092354			missense	benign	0.003	0.48	7.033	heterozygous	uc021w co.1,CEP250,+,6157C->T,0,non-syn,His2053Tyr:	
27	chr21:47746480-47746480	*PCNT*	605925	missense,5utr,regulation	benign	0.031	0.22	8.15	heterozygous	uc002zji.4,PCNT,+,244G->A,0,non-syn,Ala82Thr:	
	chr21:47817979-47817979			missense	benign	0.056 0.013	0.52	15.23	heterozygous	uc002zji.4,PCNT,+,4498C->A,0,non-syn,Gln1500Lys:	
28	chr22:29737521-29737521	*AP1B1*		missense	benign	0.192 0.06 0.128 0.139	0.25	23.1	homozygous	uc003afi.3,AP1B1,-,1765C->T,0,non-syn,Val589Met:	
29	chr22:30070914-30070914	*NF2*	607379	missense,noncoding ,intronic	benign	0.128 0.081 0.162 0.167 0.419 0.305 0.435		25.4	homozygous	uc003afy.4,NF2,+,1430C->T,1,non-syn,Thr477Ile:	not segregregating with disease
30	chr22:36122486-36122486	*APOL5*		missense	possibly damaging	0.764	0.01	23.5	homozygous	uc003aof.3,APOL5,+,371C->T,1,non-syn,Ala124Val:	not segregregating with disease

Family 3

Individual F3:II.1										
n	Chr (hg 19)	Gene	Omim	Function	pph2	pph2 prob	Sift	CADD	Variant alleles	Transcripts
1	**chr5:179250038-179250038**	***SQSTM1***	**601530**	**stopgain**				**45**	**homozygous**	**SQSTM1:NM_003900:exon2:c.C286T:p.R96X,SQSTM1:NM_001142298:exon3:c.C34T:p.R12X,SQSTM1:NM_001142299:exon3:c.C34T:p.R12X**
2	chr17:18137420-18137420	*LLGL1*		synonymous, splice region variant				10.57	homozygous	LLGL1:NM_004140:exon6:c.C645T:p.Y215Y ,(p.%3D)
3	chr19:38949938-38949938	*RYR1*	180901	missense				31	heterozygous	RYR1:NM_000540:exon19:c.G2320A:p.G774R,RYR1:NM_001042723:exon19:c.G2320A:p.G774R
	chr19:39070676-39070676			missense				22.5	heterozygous	RYR1:NM_001042723:exon99:c.A14404T:p.N4802Y ,RYR1:NM_000540:exon100:c.A14419T:p.N4807Y

Family 4

F4:II.1 and F4:II.4: Prioritized Variants Common to Both Individuals

rank score	Chr (hg 19)	Variant	Gene	Omim	Function	pph2	Sift	CADD	Variant alleles	Transcripts
27	**chr:5:179250038**	**C-T**	***SQSTM1***	**601530**	stop-gain	-	-	**45.0**	**homozygous**	**NM 001142298, NM 001142299, NM 003900**
22	chr4: 71654570	C-T	*RUFY3*	-	missense-variant	probably damaging	deleterious	34.0	heterozygous	NM 001130709, NM 001037442, NM 014961
22	chr19:15769117	G-A	*CYP4F3*	-	missense-variant	probably damaging	deleterious	26.0	heterozygous	NM 001199209, NM 001199208, XM 005259910, NM 000896
21	chr16:81697886	C-T	*CMIP*	-	missense-variant	probably damaging	tolerated	34.0	heterozygous	NM 030629, NM_198390 XM_005256179
18	chr22:36708231	C-G	*MYH9*	603622, 153650, 153640, 600208, 155100, 605249	missense-variant	probably damaging	-	25.5	heterozygous	NM 002473
18	chr16:89815066	C-T	*FANCA*	227650	splice-donor variant	-	-	25.7	heterozygous	NM_001286167 XM_005256294, NM 000135